FeedNetBack D03.05 - Networking Protocols for Control

T. Oechtering, L. Bao, Pangun Park, Jose Araujo, Carlo Fischione, Alain Kibangou, Mikael Skoglund, K.E. Johansson

▶ **To cite this version:**

T. Oechtering, L. Bao, Pangun Park, Jose Araujo, Carlo Fischione, et al.. FeedNetBack D03.05 - Networking Protocols for Control. 2011. hal-00785700

HAL Id: hal-00785700
https://hal.science/hal-00785700

Submitted on 6 Feb 2013

HAL is a multi-disciplinary open access archive for the deposit and dissemination of scientific research documents, whether they are published or not. The documents may come from teaching and research institutions in France or abroad, or from public or private research centers.

L'archive ouverte pluridisciplinaire **HAL**, est destinée au dépôt et à la diffusion de documents scientifiques de niveau recherche, publiés ou non, émanant des établissements d'enseignement et de recherche français ou étrangers, des laboratoires publics ou privés.

GRANT AGREEMENT N°223866

Deliverable	D03.05
Nature	Report
Dissemination	Public

D03.05 – Networking Protocols for Control

Report Preparation Date 31/08/2011
Project month: 36

Authors Tobias J. Oechtering, KTH, Lei Bao, KTH,
Pangun Park, KTH, Jose Araujo, KTH,
Carlo Fischione, KTH,
Alain Kibangou, INRIA,
Mikael Skoglund, KTH,
Karl Henrik Johansson, KTH

Report Version V1
Doc ID Code KTH04_R_D0305_31082011_V1

Contract Start Date : 01/09/2008
Duration : 41 months
Project Coordinator : Carlos CANUDAS DE WIT, INRIA, France

Theme 3:

Information and Communication Technologies

SUMMARY

This report documents the research work carried out for Task 3.4. on networking protocols for control. The main objective is to design and study radio networking protocols which are adapted to fit a given control application. Accordingly, most of the work deals with a resource optimization problem under the constraint of strict delay constraints and allowable packed loss rate where a high-level model of the communication network is assumed.

Three different approaches are taken. First, we optimize the instantaneous communication rate allocation for state feedback control over noisy channels using high-rate approximation theory. Second, we present a framework for the joint design of controllers and a network for multiple control systems where the sensor measurements are transmitted to the controller over the IEEE 802.15.4 wireless network, which considers the critical aspects for both control and communication systems. Lastly, we study cooperative data detection where a CDMA protocol is used for exchange information between nodes grouped in two clusters, which results in a distributed version of Alternating Least Squares algorithm using average consensus iterations.

Contents

1 Introduction

This document is the final report on the work done for *Task 3.4 – Networking protocol for Control* of the *Work package 3 – Control and Communications* of the FeedNetback project. The work in Task 3.4 considers the design of network protocols and the study of the corresponding achievable performances of the control systems where high-level models of the radio communication network are used. Radio communication increases the mobility and flexibility, but also leads to unreliable communication channels. Therefore, the main objective is the design of resource-efficient network protocols which are able to meet strict delay constraints and requirements on the allowed packed loss rate.

The need for customized networking protocols for networked control is mainly due to the fact that unreliable and delayed communication in networks can destabilize or severely restrict the performance of closed-loop systems. This means that protocols with low-delay routing and retransmission strategies have to be developed and/or adjusted. In recent years, the demand for efficient resource sharing in large networked systems has been continuously increasing. Therefore, the resource allocation needs to be optimized for efficient protocol designs. New signaling protocols and algorithms are in need to achieve the requirements imposed by control applications. Accordingly, we considered the joint design of the control strategy and the allocation communication power/rate, which is useful for the dimensioning of a network. The optimization of the joint design is performed with appropriate constraints on the packet loss probability and delay. They also provide insights about the influence of networking and routing protocols on the control performance assuming a given control strategy. Further, a cooperative data detection strategy for exchange of information between nodes of different clusters is studied.

Outline of this Document

The main body of the report consists of three parts of work regarding networking protocols for control applications.

First, in Section 2, we study the problem of optimizing instantaneous communication rate for state feedback control over a noisy channel. The proposed rate allocation method is composed of two steps: (i) the overall performance measure is expressed as a function of rates at all time instants by means of high-rate quantization theory, and (ii) a constrained optimization problem to maximize the

performance is solved by means of Lagrange duality theory. It is shown that the proposed method has better performance when compared to arbitrarily selected rate allocations.

Second, in Section 3, we present a framework for the joint design of controllers and a network for multiple control systems where the sensor measurements are transmitted to the controller over the IEEE 802.15.4 wireless network. The design approach relies on a constrained optimization problem, whereby the objective function is the energy consumption of the network and the constraints are the packet loss probability and delay. After presenting the analytical model of the packet loss probability and delay of the network, we apply Linear Quadratic Gaussian (LQG) control and derive the cost as a function of the packet loss probability and delay.

Lastly, in Section 4, we study cooperative data detection where a CDMA protocol is used for exchanging information between nodes grouped in two clusters. In particular, we consider communication over multiple access fading channels. The result is a distributed version of Alternating Least Squares (ALS) algorithm using average consensus iterations. A numerical study is performed to compare the performance of the proposed distributed ALS algorithm with the traditional ALS algorithm.

Finally, we provide a collection of conclusions of each study in Section 5.

2 Optimized rate allocation for closed-loop control over noisy channels

In this section we study the problem of optimizing communication rate for state feedback control over a noisy channel. Linear dynamic systems with quantization errors, limited transmit powers, and noisy communication channels are considered. The most challenging part of the analysis is that no closed-form expressions are available for assessing the performance and the optimization is non-convex. The proposed method consists of two steps: (i) the overall performance measure is expressed as a function of rates at all time instants by means of high-rate quantization theory, and (ii) a constrained optimization problem to maximize the performance is solved. It is shown that non-uniform quantization is in general the best strategy for feedback control over noisy channels. It is also shown that the proposed method has better performance when compared to arbitrarily selected rate allocations.

Outline: In Section 2.1 a brief motivation of the rate allocation problem is provided. In Section 2.2 we define the control system with encoder, controller, and communication channel. Thereafter, the problem statement which concerns rate allocation for closed-loop control is formulated. In Section 2.3 we describe the solution based on high-rate theory and Lagrange methods. Finally, we present numerical experiments in Section 2.4 and conclusions in Section 2.5.

2.1 Background

Networked control systems (NCS) based on limited sensor and actuator information have attracted increasing attention during the past decade (Luo and Liu 2006, Willig 2008). In future NCSs, the monitoring and control tasks could be performed by simple, inexpensive, and small sensor nodes, which means that the transmitting and the computing power are highly limited. How to optimize the use of resources to provide sustained overall system performance is an important aspect for well-designed networking protocols. In digital communication systems, the power consumption is determined by two factors: the amount of information to transmit, i.e., the communication rate, and the power used for transmission. Hence, the selection of communication rate is an essential part of protocol design for networks subject to power constraints.

To utilize the limited communication resources efficiently, it is especially in-

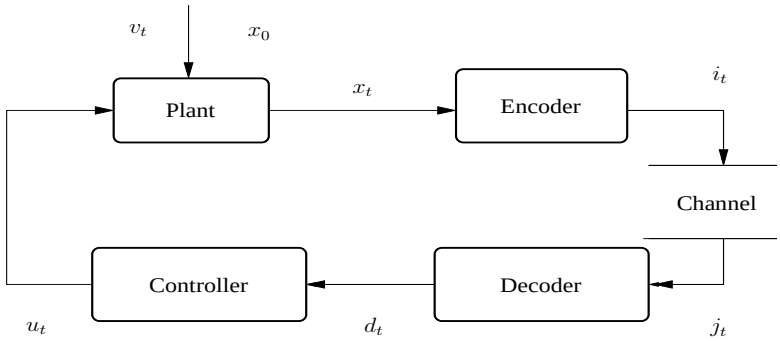

Figure 1: Block-diagram for the closed-loop system. The system has a separate decoder unit and a controller.

teresting to study the case where the sensed data is quantized by using few bits so to reduce the amount of information to transmit. This is achieved by transmitting few possible symbols with each symbol consisting of few bits. Besides reducing the energy power consumption, there is another advantage in constraining the bit resolution per transmission: It allows for low latency in the decoding. Owing to the non-stationarity of the state observations, an even distribution of bits over time to sensor measurements is often not efficient for networked control. It is natural to expect considerable gains by employing a non-uniform allocation of radio powers and rates. Hence, optimizing the rate allocation is vital to overcome the limited communication resources and to achieve a better overall control and communication performance.

Allocating communication resources over space and time is important. For feedback control systems this is a largely open problem. How to assign bits among the elements of the state of the plant, while imposing a constraint on the available transmit power, can be found in, e.g., (Ling and Lemmon 2005, Xiao, Johansson, Hindi, Boyd and Goldsmith 2005). The rate allocation problem studied in this work is related to classical rate allocation problems in communications, e.g., (Gersho and Gray 1992, Farber and Zeger 2006), where high-rate quantization theory is used to quantify the relation between rate and performance.

2.2 System Description and Problem Statement

Consider the control system with a communication channel depicted in Fig. 1. The scalar plant is governed by the linear equation

$$x_{t+1} = ax_t + u_t + v_t, \tag{1}$$

where $x_t, u_t, v_t \in \mathbb{R}$ denote plant state, control input and process noise, respectively. Process noise v_t is modeled as an i.i.d. zero-mean Gaussian process with a variance σ_v^2. It is mutually independent of the initial state x_0, which is also i.i.d. zero-mean Gaussian with a variance $\sigma_{x_0}^2$.

At the encoder, the full state measurement is coded by a memoryless time-varying encoder, which takes the current state x_t as the input, and produces an index i_t,

$$i_t = f_t(x_t, R_t), \tag{2}$$

where $R_t \in \mathbb{Z}^+$ denotes the time-varying instantaneous rate. We introduce the index set $\mathcal{L}_t(R_t) = \{0, \ldots, 2^{R_t} - 1\} \subseteq \mathbb{Z}^+$, and for a given R_t, $i_t \in \mathcal{L}_t$.

The overall channel, composed by the combination of the random index assignment and a binary symmetric channel (BSC), is completely specified by the symbol transition probabilities $\Pr(j_t | i_t)$, with $j_t \in \mathcal{L}_t$ denoting the received index. At the bit level, the channel is characterized by the crossover probability $\epsilon = \Pr(0|1) = \Pr(1|0)$ of the BSC. The overall symbol error probability $\Pr(j_t|i_t)$ is determined by both ϵ and the randomized IA, according to

$$\Pr(j_t | i_t) = \begin{cases} \alpha(R_t), & j_t \neq i_t, \\ 1 - (2^{R_t} - 1)\alpha(R_t), & j_t = i_t, \end{cases} \tag{3}$$

where $\alpha(R_t) \triangleq (1-(1-\epsilon)^{R_t})/(2^{R_t}-1)$ is obtained by averaging over all possible IA's (Zeger and Manzella 1994).

At the receiver side, there is a separate decoder unit and a controller. The decoder takes the instantaneous channel output j_t as the input, and produces an estimate of x_t, denoted by d_t,

$$d_t = D_t(j_t) \in \mathbb{R}, \tag{4}$$

where $D_t(\cdot)$ is a deterministic function. The estimate d_t can take on one of 2^{R_t} values, referred to as the reconstructions. Finally, the control u_t is computed based on the decoded symbol, $u_t = g_t(d_t) \in \mathbb{R}$.

The objective is to minimize the expected overall cost $\mathbf{E}\{J_{\text{tot}}(\mathbf{R})\}$, $\mathbf{R} = \{R_0, \ldots, R_{T-1}\}$, over a finite horizon, subject to the total transmit radio power

constraint $\sum_{t=0}^{T-1} R_t P \leq P_{\text{tot}}$, $R_t \in \mathbb{Z}^+$, with P denoting the radio power consumption per bit, and P_{tot} denoting the total power available. The constraint can be readily rewritten as $\sum_{t=0}^{T-1} R_t \leq R_{\text{tot}}$, with $R_{\text{tot}} = P_{\text{tot}}/P$. The overall cost $J_{\text{tot}}(\mathbf{R})$ is given as

$$J_{\text{tot}}(\mathbf{R}) = \sum_{t=0}^{T-1} J_t(\mathbf{R}_t) = \sum_{t=1}^{T} x_t^2 + \rho u_{t-1}^2, \quad \rho \geq 0. \tag{5}$$

We are restricted to use the following linear control policy

$$u_t = \ell_t d_t, \tag{6}$$

where ℓ_t is defined as

$$\ell_t \triangleq -\frac{a\phi_{t+1}}{\phi_{t+1} + \rho}, \quad \phi_t \triangleq 1 + \frac{a^2 \phi_{t+1} \rho}{\phi_{t+1} + \rho}, \quad \phi_T = 1. \tag{7}$$

The motivation of (6) can be found in (Bao, Skoglund, Fischione and Johansson 2010). Therewith, minimizing $\mathbf{E}\{J_{tot}(\mathbf{R})\}$ of (5) is equivalent to minimizing the expected value of

$$J_{\text{tot}}(\mathbf{R}) = \sum_{t=0}^{T-1} \pi_t (x_t - d_t)^2, \quad \pi_t \triangleq (\phi_{t+1} + \rho)\ell_t^2. \tag{8}$$

Summarizing the above discussions, Problem 1 below specifies the rate allocation problem for state feedback control studied in this work.

Problem 1. *Given a linear plant of* (1)*, a discrete memoryless channel of* (3)*, a memoryless encoder–decoder pair of* (2) *and* (4)*, subjected to the linear control law* (6)*, find the optimal bit-rate allocation* $\mathbf{R}$ *which minimizes the expected objective function* (5)*, subject to the total bit constraint, i.e.,*

$$\begin{array}{ll} \min\limits_{\mathbf{R}} & \sum_{t=0}^{T-1} \pi_t \mathbf{E}\left\{(x_t - d_t)^2\right\}, \\ \text{s.t.} & \sum_{t=0}^{T-1} R_t \leq R_{\text{tot}}, \quad R_t \in \mathbb{Z}^+, \quad \forall t. \end{array}$$

2.3 Rate Allocation for State Feedback Control

First, we are interested in an efficient approximation to describe the relation between the MSE $\mathbf{E}\{(x_t - d_t)^2\}$ and the rate R_t. By using high-rate theory, we

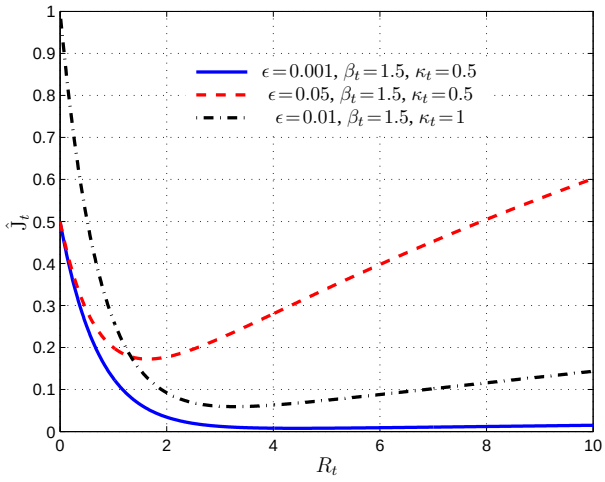

Figure 2: The impact of R_t, κ_t, β_t and ϵ on the objective function $\hat{\mathrm{J}}_t$.

approximate the MSE by $\hat{\mathrm{J}}_t$ as follows,

$$\begin{aligned}\mathbf{E}\left\{(x_t-d_t)^2\right\} &\approx \hat{\mathrm{J}}_t(\beta_t,\kappa_t,R_t) \triangleq \beta_t(1-(1-\epsilon)^{R_t})+\kappa_t 2^{-2R_t},\\ \beta_t &\triangleq \sigma_{x_t}^2+\int_y y^2\lambda_t(y)\mathrm{d}y,\\ \kappa_t &\triangleq \frac{G^{-2}}{3}\int_x \lambda_t^{-2}(x)p(x_t=x)\mathrm{d}x,\end{aligned} \tag{9}$$

where, the constant G represents the volume of a unit sphere. The function $\lambda_t(x)$ is referred to as the point density function, specifying the density of reconstructions of the quantizer. As shown in (Bao et al. 2010), (9) is a quasi-convex function in R_t, see Fig. 2. In particular, we are interested in the class of $\hat{\mathrm{J}}_t$, which can be decomposed as

$$\hat{\mathrm{J}}_t(\beta_t,\kappa_t,R_t)=\sigma_x^2\tilde{\mathrm{J}}_t(\tilde{\beta}_t,\tilde{\kappa}_t,R_t)=\sigma_{x_t}^2\left(\tilde{\beta}_t(1-(1-\epsilon)^{R_t})+\tilde{\kappa}_t 2^{-2R_t}\right). \tag{10}$$

In order to express the instantaneous objective function in terms of all past communication rates, we will further approximate x_t by a zero-mean Gaussian source $\mathrm{N}(0,\hat{\sigma}_{x_t}^2)$, because the initial state and the process noise are zero-mean Gaussian. Moreover, we let the variance $\hat{\sigma}_{x_t}^2$ evolve according to

$$\hat{\sigma}_{x_t}^2=(A_t+B_t\tilde{\mathrm{J}}_{t-1}(\tilde{\beta}_{t-1},\tilde{\kappa}_{t-1},R_{t-1}))\hat{\sigma}_{x_{t-1}}^2+\sigma_v^2, \tag{11}$$

where $A_t > 0$ and $B_t > 0$ are independent of R_{t-1}, $\hat{\sigma}^2_{x_{t-1}}$ and σ_v^2. Next, we present one of our main results.

Theorem 1. - *For error-free channels* ($\epsilon = 0$)*, it holds that a solution* $\mathbf{R} \in \mathbb{R}^T$ *to the system*

$$\begin{aligned} \sum_{s=t}^{T-1} \left(2 \sum_{b_0=0}^{1} \cdots \sum_{b_t=1}^{1} \cdots \sum_{b_{s-1}=0}^{1} \Psi_s(\mathbf{b}_0^{t-1}) \right) &= \theta, \quad \forall t, \\ \sum_{t=0}^{T-1} R_t &= R_{\text{tot}}, \end{aligned} \tag{12}$$

solves the constrained rate allocation problem, with θ *being the associated Lagrange multiplier, and*

$$\Psi_t(\mathbf{b}_0^{t-1}) \triangleq \pi_t \bar{B} \left(\prod_{s=\bar{s}+1}^{t-1} \bar{B}_s \right) \left(\prod_{m=0}^{t} \tilde{\kappa}_m^{b_m} \right) 2^{-2\left(\sum_{n=0}^{t-1} b_n R_n + R_t\right)}. \tag{13}$$

1. π_t *and* $\tilde{\kappa}_t$ *are specified in* (8) *and* (10)*.*
2. $\bar{s}$ *is the smallest integer* s *such that* $b_s = 1$*.*
3. *The term* $\bar{B}$ *is defined as*

$$\bar{B} \triangleq \begin{cases} \tau_{\bar{s}-1}, & \bar{s} > 0, \\ B_0 \sigma_{x_0}^2, & \bar{s} = 0, \end{cases} \tag{14}$$

   where τ_s *is calculated recursively as*

$$\tau_s \triangleq A_s \tau_{s-1} + \sigma_v^2, \quad \tau_0 \triangleq A_0 \sigma_{x_0}^2 + \sigma_v^2.$$

4. *The term* $\bar{B}_s$ *is chosen between* A_s *and* B_s*, determined by* b_s*,*

$$\bar{B}_s \triangleq \begin{cases} A_s, & b_s = 0, \\ B_s, & b_s = 1. \end{cases} \tag{15}$$

- *For noisy channels* ($\epsilon \neq 0$)*, it follows that*

1. *If* $R_{\text{tot}} \geq \sum_{t=0}^{T-1} R_t^\star$*, where* $\mathbf{R}^\star$ *solves the system of equations*

$$\frac{\partial \tilde{\mathrm{J}}_t}{\partial R_t}(\tilde{\beta}_t, \tilde{\kappa}_t, R_t^\star) = 0, \quad \forall t, \tag{16}$$

   with $\tilde{\mathrm{J}}_t(\tilde{\beta}_t, \tilde{\kappa}_t, R_t)$ *given by* (10)*, then the same* $\mathbf{R}^\star$ *solves the constrained rate allocation problem.*

2. *If* $R_{\text{tot}} < \sum_{t=0}^{T-1} R_t^\star$, *where* $\mathbf{R}^\star$ *is a solution to* (16)*, then the solution to the system of equations*

$$\begin{aligned} -\sum_{s=t}^{T-1} \Psi_{t,s} &= \theta, \quad \forall t, \\ \sum_{t=0}^{T-1} R_t &= R_{\text{tot}}, \end{aligned} \tag{17}$$

solves the constrained optimization problem. Here, the term $\Psi_{t,s}$ *is*

$$\Psi_{t,s} \triangleq \sum_{b_0=0}^{1} \cdots \sum_{b_t=1}^{1} \cdots \sum_{b_{s-1}=0}^{1} \pi_s \bar{\Psi}(\mathbf{b}_0^s), \tag{18}$$

where $b_k \in \{0,1\}$, $k \in \mathbb{Z}^+$, *and*

$$\bar{\Psi}(\mathbf{b}_0^s) \triangleq \bar{B} \left(\prod_{m=\bar{s}+1}^{s-1} \bar{B}_m \right) \left(\prod_{n=\bar{s}+1}^{s} C_n^{b_n} \right).$$

The terms $\bar{B}$ *and* $\bar{B}_n$ *are as given by* (14)–(15)*, and* C_n *is defined as*

$$C_n \triangleq \begin{cases} \frac{\partial \tilde{\mathrm{J}}_n}{\partial R_n}(\tilde{\beta}_n, \tilde{\kappa}_n, R_n), & n = t, \\ \tilde{\mathrm{J}}_n(\tilde{\beta}_n, \tilde{\kappa}_n, R_n), & n \neq t. \end{cases} \tag{19}$$

Theorem 1 is proved by using Lagrange duality theory, as detailed in (Bao et al. 2010).

2.4 Numerical Experiments

In this section, we present numerical experiments to verify the performance of the proposed bit-rate allocation algorithm.

In Fig. 3 we demonstrate the performance of the proposed scheme, denoted by RA_{12}, by comparing it with 13 other allocations, denoted by RA_1–RA_{11}, RA_{13}, and RA_{14}. All 14 allocations are listed in the same figure. Regarding the optimized allocation, R_t is fairly evenly distributed over t, and compared with the uniform allocation RA_6, there is certain performance improvement. The uniform allocations RA_1–RA_8 have a time-invariant rate from 8 bits to 1 bit. Among these allocations, RA_8, for which $R_t = 1$, $\forall t$, has the worst performance, while RA_4, for which $R_t = 5$, $\forall t$, has the best performance. In fact, based on our analysis,

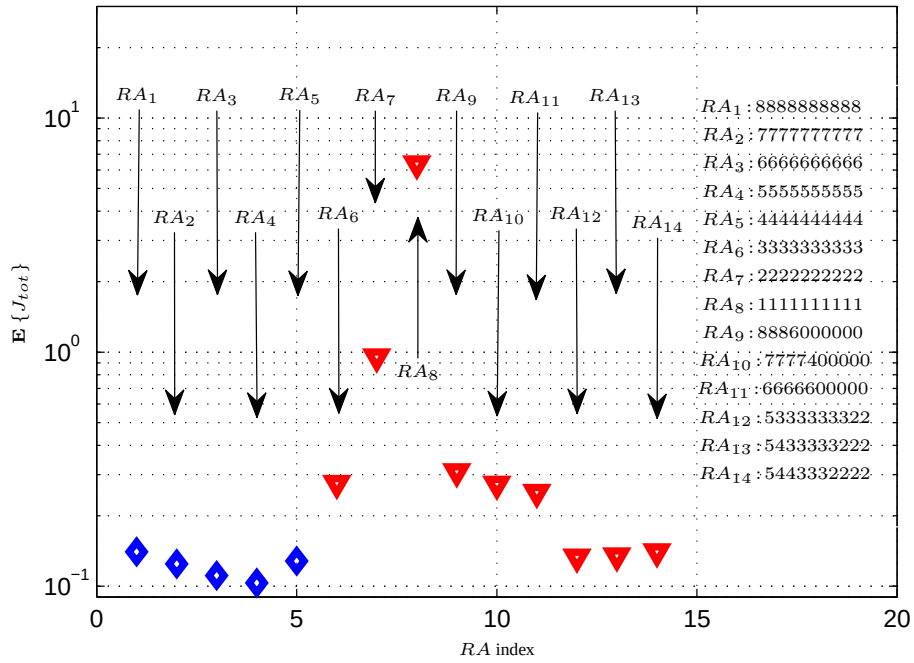

Figure 3: Performance comparison among various rate allocations for state feedback control. An allocation is the total rate constraint $\sum_{t=0}^{T-1} R_t > 30$. Allocations marked with a triangle fulfill the total rate constraint, $\sum_{t=0}^{T-1} R_t \leq 30$.

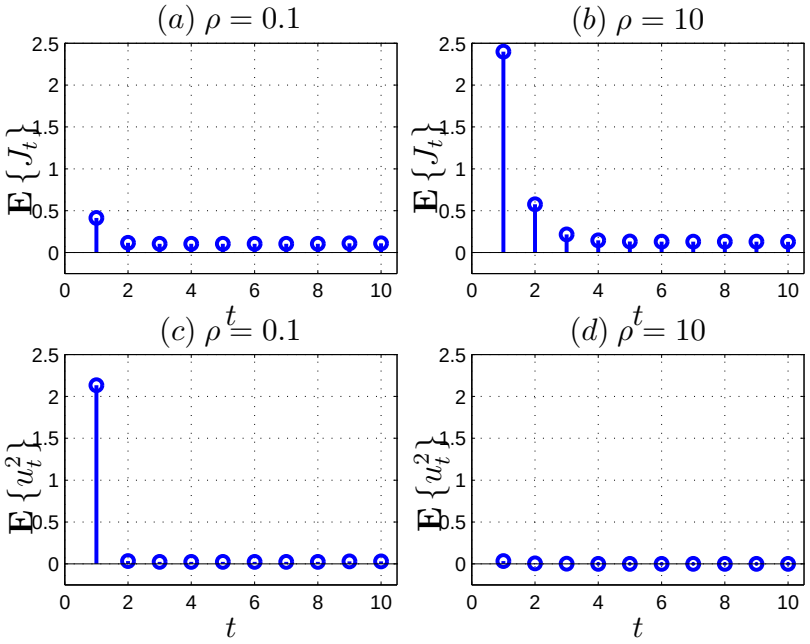

Figure 4: Performance comparison between $\rho = 0.1$ and $\rho = 10$.

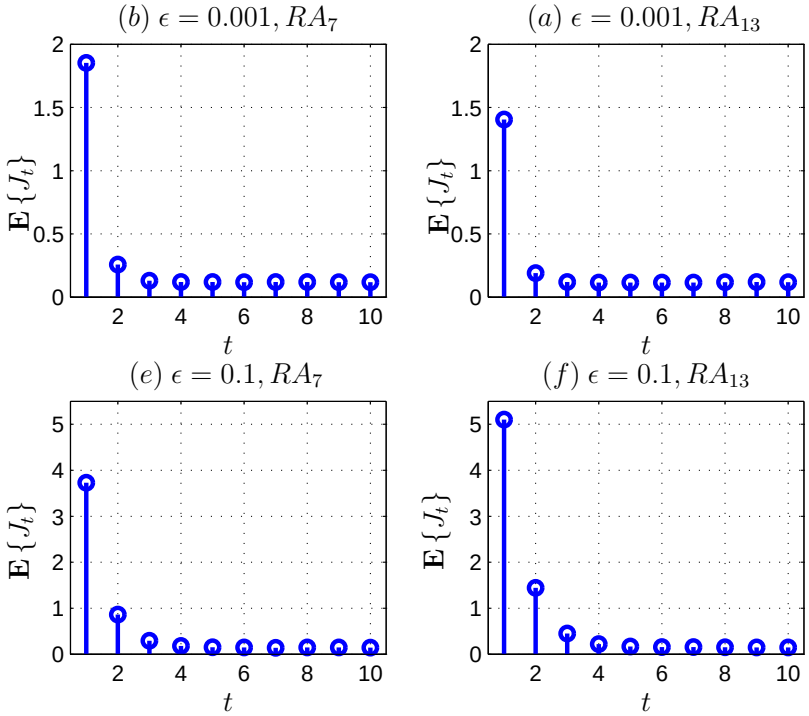

Figure 5: Performance comparison with respect to ϵ.

the solution to the unconstrained rate allocation problem is RA_4, i.e., $R_t^\star = 5, \forall t$. This is consistent with the simulation result that RA_5 is superior to allocations that are assigned more than 5 bits for every t, cf., RA_1–RA_3.

The purpose of the next example is to demonstrate the impact of the crossover probability ρ. The weighting parameter ρ plays a role of regulating the power of the control signal. The simulated instantaneous costs for $\rho = 0.1$ and $\rho = 10$ are depicted in Fig. 4. The optimized rate allocations are $RA_{12} = \{5333333322\}$ and $RA_{14} = \{5443322222\}$ for $\rho = 0.1,\ 10$, respectively. When ρ is small, for example $\rho = 0.1$, large-valued controls are allowed and the steady state is quickly reached. As ρ increases, only small-valued controls are allowed and it takes longer time to reach the steady state. This explains RA_{14} that more bits are needed in the initial states when ρ is large.

In Fig. 5, the impact of the parameter ϵ is studied. Applying Theorem 1, we obtain RA_{13} for $\epsilon = 0.001$, and RA_7 for $\epsilon = 0.1$, respectively. At $\epsilon = 0.001$, the global minimum to the unconstrained problem is $R_t^\star = 5$, which means the rate constraint is violated at the global minimum. On the other hand, at $\epsilon = 0.1$, the global minimum is $R_t = 2$, so the rate constraint applies.

Finally, the Gaussian approximation becomes less accurate as the significance of control increases, which is assessed below by a numerical example. In Fig. 6, a comparison of the PDF's of the estimated x_t and the true x_t is depicted, for two ρ values: $\rho = 0.1$ and $\rho = 1$. We could observe that for large-valued ρ, the influence of control is moderate. Consequently, the system behaved more like the open-loop system. Therefore the Gaussian assumption is more accurate. On the other hand, for small-valued ρ, the influence of control is significant, which reduces slightly the accuracy of the Gaussian assumption of the state x_t. We conclude that the assumption works well in practice.

2.5 Conclusion

We have proposed a new method to optimize the allocation of radio resources in control over wireless channels. In order to arrive at a tractable objective function, we first approximated the objective functions by means of the high-rate approximation theory. Then we solved the rate constrained optimization problems by means of Lagrangian duality for non-convex problems.

Currently, we have extended the rate allocation problem to the scenario with multiple plants. In the preliminarily study, two objective functions have been considered. The first one is the sum of the costs of all the plants, and this formulates a single-objective function. The second one is given by a vector consists of the costs

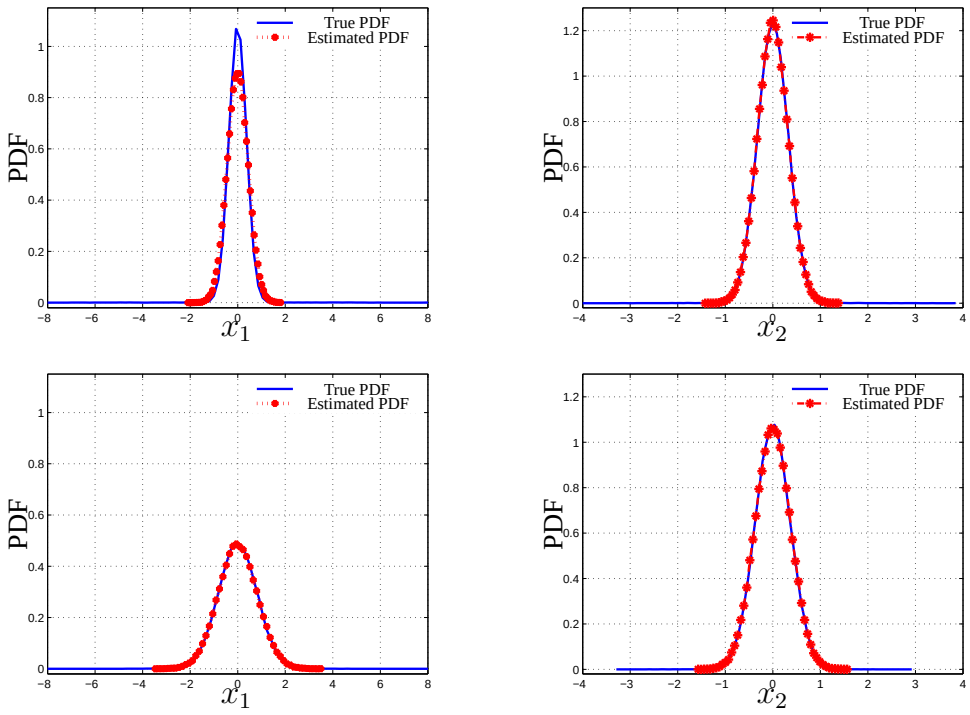

(c) $\rho = 1$ (d) $\rho = 1$

Figure 6: The PDF's of the estimated x_t and the true x_t, $t = 1, 2$, for two ρ values.

of all the plants, and it formulates a multi-objective function. The single-objective optimization problem has been solved following the solution to the single plant scenario. The multi-objective optimization problem has been solved by using the Pareto approach.

3 Joint design of controllers and a network for multiple control systems

There are major advantages in terms of increased productivity and reduced installation costs in the use of wireless communication technology in industrial control systems (Willig 2008, Park 2009). The IEEE 802.15.4 standard has received considerable attention as a low data rate and low power protocol for Wireless Sensor Network (WSN) applications in industry, control, home automation, health care, and smart grids (Willig 2008, Park 2009, IEE 2006).

Although WSNs provide a great advantage for the process and manufacturing industries, they are not yet efficiently deployed. One of the most significant reasons is the lack of proper modelling of the network behavior. Any wireless networks introduce random packet losses and delays due to the harsh nature of the wireless channel, limited bandwidth, and interference generated by other wireless devices because of unlicensed spectrum bands. The tradeoff between tractability and accuracy of the analytical model of a wireless network is important in order to hide the system complexity through a suitable abstraction without losing critical aspects of the network. Furthermore, WSNs require energy-efficient operation due to the limited battery power of each sensor node. Research to achieve high performance of control systems through a communication network has been proposed. The approach can be grouped in two categories: design of the control algorithm and design of the communication protocol. Some research has been done in designing robust controllers and estimators that are adaptive and robust to the communication faults: packet delay (Nilsson 1998b, Nilsson 1998a), packet dropout as a Bernoulli random process (Seiler and Sengupta 2001, Sinopoli, Schenato, Franceschetti, Poolla, Jordan and Sastry 2004) or with deterministic rate (Yu, Wang, Xie and Chu 2004), and data rate limitation (Nair, Fagnani, Zampieri and Evans 2007). Communication protocols or parameters are designed in order to achieve a given control performance. In (Henriksson and Cervin 2005), the authors present a scheduling policy to minimize a LQ cost under computational delays. In (Liu and Goldsmith 2004), the authors proposed an adaptive tuning scheme of the parameters of the link layer, MAC layer and sampling period through numerical results in order to minimize the LQ cost. However, these papers often consider only one aspect of the network faults: packet delay (Nilsson 1998b, Nilsson 1998a, Henriksson and Cervin 2005), packet dropout (Seiler and Sengupta 2001, Sinopoli et al. 2004, Yu et al. 2004), or data rate limitation (Nair et al. 2007). In (Liu and Goldsmith 2004), although the authors

consider the simulation results of the wireless network, the framework has not been designed out of an analytical consideration of control performance.

In this report we summarize two original contributions:

1. We investigate the achievable networked control performance by considering a realistic model of the wireless network.

2. We propose a co-design approach to meet the required control performance while minimizing the energy consumption of the network.

In particular, the co-design approach is based on a constrained optimization problem, whereby the objective function is the energy consumption of the wireless network and the constraint is the desired control performance. The network model is based on our recent research in (Park, Marco, Soldati, Fischione and Johansson 2009). The key issue is how to derive the explicit relation between the performance of the control systems and the characteristics of a wireless network. Furthermore, the well-defined design procedure is required in order to achieve the high performance of networked control systems.

The outline of this section is as follows. Section 3.1 defines the considered problem of control over a wireless network. In Section 3.2, we describe the IEEE 802.15.4 standard and its network model. Then, the design of the estimator and the controllers is presented in Section 3.3. In Section 3.4, we propose the co-design approach and illustrate it through numerical examples. In addition, we show the achievable control performance over the IEEE 802.15.4 standard. Section 3.4.3 concludes this work.

3.1 Problem Formulation

The problem considered is depicted in Fig. 7, where multiple linear systems are controlled over a WSN using the IEEE 802.15.4 MAC standard. All M plants contend to transmit sensor measurements to the controller over a wireless network which induces packet losses and varying delays. We assume that a sensor node is attached to each plant. A contention-based IEEE 802.15.4 MAC protocol is used to determine which sensor node sends a packet. Throughout this section we consider control applications where nodes asynchronously generate packets when a timer expiries. When a node sends a packet successfully or discards a packet, the node stays in the idle period for $\overline{h}$ seconds without generating packets. The data packet transmission is successful if an acknowledgement (ACK) packet is

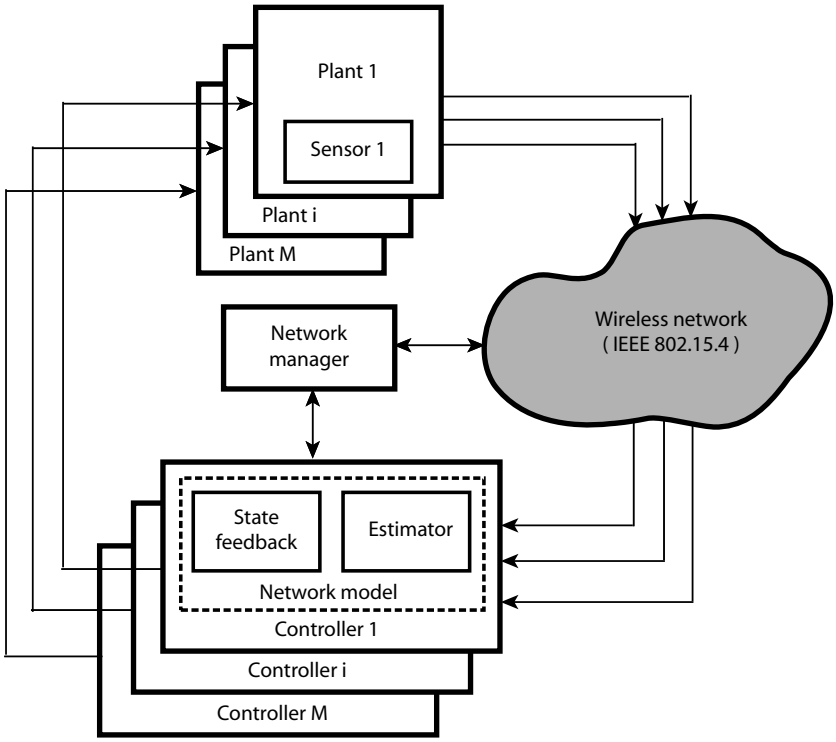

Figure 7: Overview of the networked control system setup. M plants need to be controlled by M controllers. The wireless network closes the loop from the sensor nodes to the controllers.

received. We assume that the controller commands are always received by the actuator reliably.

More precisely, we consider a plant i given by a linear stochastic differential equation

$$dx(t) = Ax(t)dt + Bu(t)dt + dw(t) \tag{20}$$

where $x(t) \in \mathbb{R}^n$ is the plant state and $u(t) \in \mathbb{R}^m$ is the control signal. The process disturbance $w(t) \in \mathbb{R}^n$ has a mean value of zero and uncorrelated increments, with incremental covariance $R_w dt$. We neglect the plant index i to simplify notation. Let us consider the sampling of the plant with time-varying sampling period $h_k = t_{k+1} - t_k$ and delay τ_k (Aström and Wittenmark 1997). The sampling period is $h_k = \overline{h} + \tau_k$ where the idle period $\overline{h}$ is constant and the random delay is τ_k, which is bounded $\tau_k \leq \tau_{\max}$. We assume that the random sequences $\{\tau_k\}$ and $\{h_k\}$ are bounded, $0 < \tau_k < h_k$ and $0 < h_{\min} \leq h_k \leq h_{\max}$. In addition, they are stochastic, independent, and have known distributions. Notice that the networked induced delay τ_k is less than h_k and allows the packets to arrive at the controller in the correct order. By considering zero-order-hold, a time-varying discrete-time system is obtained

$$\begin{aligned} x_{k+1} &= \Phi_k x_k + \Gamma_0^k u_k + \Gamma_1^k u_{k-1} + w_k \\ y_k &= Cx_k + v_k \end{aligned} \tag{21}$$

where $\Phi_k = e^{Ah_k}$, $\Gamma_0^k = \left[\int_0^{h_k - \tau_k} e^{As} ds\right] B$, $\Gamma_1^k = \left[\int_{h_k - \tau_k}^{h_k} e^{As} ds\right] B$, and v_k is a discrete-time white Gaussian noise with zero mean and variance R_v. The k is the discrete time index. The initial state x_0 is white Gaussian with mean $\bar{x}_0$ and covariance P_0.

Packet loss is first modelled as a random process whose parameters are related to the behavior of the network. The measurement at the controller side is given by

$$\hat{y}_k = \begin{cases} Cx_k + v_k\,, & \gamma_k = 1\,, \\ 0\,, & \gamma_k = 0\,, \end{cases} \tag{22}$$

where γ_k is a Bernoulli random variable with $\Pr(\gamma_k = 1) = 1 - p$, where p is the packet loss probability which models the packet loss between the sensor and the controller.

By considering both the packet loss and delay induced by a wireless network, we introduce an augmented discrete-time state variable $z_k = \begin{pmatrix} x_k & u_{k-1} \end{pmatrix}^T$ in

order to analyze the system. The augmented state space is

$$\begin{aligned} z_{k+1} &= \Phi_d z_k + \Gamma_d u_k + w_k \\ \hat{y}_k &= \gamma_k y_k \end{aligned} \tag{23}$$

where $\Phi_d = \begin{pmatrix} \Phi & \Gamma_1 \\ 0 & 0 \end{pmatrix}, \Gamma_d = \begin{pmatrix} \Gamma_0 \\ \mathbf{I} \end{pmatrix}$ and $C_d = \begin{pmatrix} C & \mathbf{0} \end{pmatrix}$.

In this section, we investigate the co-design for meeting the requirement of control performance while minimizing the energy consumption of the network. In Fig. 7, we introduce the network manager block in order to achieve more efficient design for control systems closed by a wireless network. Particularly, the network manager requires an efficient analytical model of the packet loss and delay (i.e., between the sensors and controller) of a wireless network. Then, this model is used to design the estimator and controller that compensates for the packet loss and delay induced by the wireless network. The network manager formulates a constrained optimization problem where the objective function, denoted by E_{tot}, is the total energy consumption of the wireless network and the constraint is the requirement of control performance. Hence, the constrained optimization problem of the control system is

$$\min_{h,\mathbf{V}} \quad E_{\text{tot}}(h, \mathbf{V}, \Delta) \tag{24a}$$

$$\text{s.t.} \quad J(h, p(h, \mathbf{V}, \Delta), \tau(h, \mathbf{V}, \Delta)) \leq J_{\text{req}}\,. \tag{24b}$$

The decision variable h is the sampling period and $\mathbf{V}$ are the protocol parameters of the network. Δ includes the parameters of the network setup such as a network topology, length of packet, and number of nodes. $J(h, p(h, \mathbf{V}, \Delta), \tau(h, \mathbf{V}, \Delta))$ is the control cost, which is a function of the sampling period h, packet loss probability p, and delay τ of the network, and J_{req} is the desired maximum control cost. Notice that the packet loss probability and delay is also a function of the sampling period h, protocol parameters $\mathbf{V}$ and parameters of the network setup Δ. In (24b), the decision variables are feasible if it satisfies a given control cost J_{req}. Note that it is possible to pose different optimization problems. Suppose that the quality of control performance is the most important design criterion and the sensor nodes have a wired power supply. Then, one would want to minimize the control cost by considering the performance of the wireless network.

The problem we consider in this section is how to determine the optimal sampling period h of control systems and the protocol parameters $\mathbf{V}$ of the wireless network. We pose this as an optimization problem. In the following section,

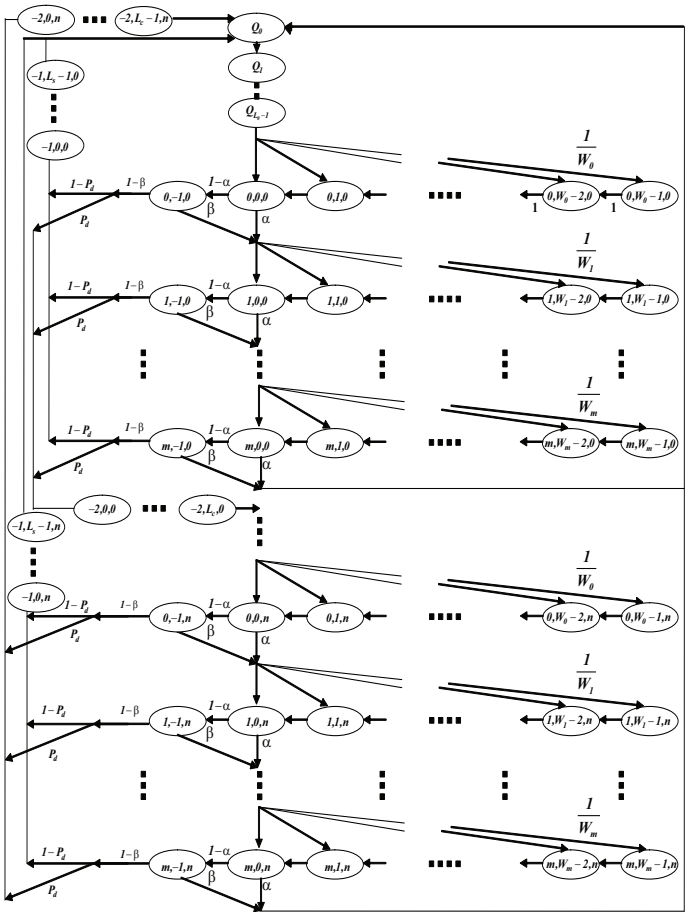

Figure 8: Markov chain model proposed in (Park et al. 2009) for the CSMA/CA algorithm of the IEEE 802.15.4 standard.

we first introduce the analytical model of the energy consumption, packet loss probability, and delay induced by the wireless network. Then, we derive the performance indicator of the controller as a function of the packet loss probability and delay in Section 3.3.

3.2 Wireless Medium Access Control Protocol

In this section, we introduce the effective analytical model of packet loss probability and delay of the wireless network imposed by the IEEE 802.15.4 standard which was originally derived in (Park et al. 2009). We first present the overview

of the carrier sense multiple access with collision avoidance (CSMA/CA) mechanism of the IEEE 802.15.4 standard. Then, we describes the analytical modelling of the wireless network based on a Markov chain model.

The contention-based MAC protocol of the IEEE 802.15.4 standard is used for control systems in this section. Consider a node trying to transmit. In the slotted CSMA/CA algorithm, first the MAC sub-layer of the node initializes four variables, i.e., the number of backoffs (NB=0), contention window (CW=2), backoff exponent (BE=*macMinBE*), and retransmission times (RT=0). Then the MAC sub-layer delays for a random number of complete backoff periods in the range $[0, 2^{\mathrm{BE}} - 1]$ units. When the backoff period is zero, the node performs the first clear channel assessment (CCA). If two consecutive CCAs are idle, then the node commences the packet transmission. If either of the CCA fails due to a busy channel, the MAC sublayer will increase the value of both NB and BE by one up to a maximum value *macMaxCSMABackoffs* and *macMaxBE*, respectively. Hence, the value of NB and BE depend on the number of CCA failures of a packet. Once the BE reaches *macMaxBE*, it remains at the value of *macMaxBE* until it is reset. If NB exceeds *macMaxCSMABackoffs*, then the packet is discarded due to the channel access failure. Otherwise the CSMA/CA algorithm generates a random number of complete backoff periods and repeat the process. Here, the variable *macMaxCSMABackoffs* represents the maximum number of times the CSMA/CA algorithm is required to backoff. If channel access is successful, the node transmits the frame and waits for ACK. The reception of the corresponding ACK is interpreted as successful packet transmission. If the node fails to receive ACK due to collision or ACK timeout, the variable RT is increased by one unit up to *macMaxFrameRetries* units. If RT is less than *macMaxFrameRetries*, the MAC sublayer initializes two variables CW=0, BE=*macMinBE* and follows the CSMA/CA mechanism to re-access the channel. Otherwise the packet is discarded due to the retry limits. See (IEE 2006) for further details.

In such a scenario, a precise and effective analytical model of the slotted CSMA/CA of the IEEE 802.15.4 standard was proposed in (Park et al. 2009). It is modelled through a Markov chain taking into account retry limits, acknowledgements, unsaturated traffic load, and the parameters of the network setup such as a length of packet and number of nodes. Let $s(t), c(t)$ and $r(t)$ be the stochastic process representing the backoff stage, the state of the backoff counter and the state of retransmission counter at time t, respectively, experienced by a node to transmit a packet, as indicated in the Fig. 8. By assuming that nodes start sensing independently, the stationary probability μ that the node attempts a first carrier sensing in a randomly chosen slot time is constant and indepen-

dent of the other nodes. It follows that (s, c, r) results in a three dimensional Markov chain with the time unit *aUnitBackoffPeriod* (corresponding to 0.32 ms). The MAC parameters are denoted by $W_0 = 2^{macMinBE}, m_0 = \textit{macMinBE}, m_b = \textit{macMaxBE}, m = \textit{macMaxCSMABackoffs}, n = \textit{macMaxFrameRetries}$. The states from $(i, W_m - 1, j)$ to $(i, W_0 - 1, j)$ represent the backoff states. States $(Q_0, \ldots, Q_{L_0-1})$ consider the idle state that the packet queue is empty and the node is waiting for a new packet arrival. The idle states $(Q_0, \ldots, Q_{L_0-1})$ take into account the unsaturated traffic condition with $\bar{h} = L_0 \times \textit{aUnitBackoffPeriod}$. States $(i, 0, j)$ and $(i, -1, j)$ represent the first channel assessment (CCA_1) and second assessment (CCA_2), respectively. α is the probability that CCA_1 is busy, and β is the probability that CCA_2 is busy. States $(-1, k, j)$ and $(-2, k, j)$ consider the successful transmission and packet collision. Note that P_d is the packet collision probability and L_s and L_c are the successful transmission time and the packet collision time, respectively. The probability μ that a node attempts CCA_1 and the busy probabilities α and β are derived by solving the state transition probabilities associated with the Markov chain model.

The precise model gives us the objective function, energy consumption (24a), and the packet loss probability and delay in a numerical form in (Park et al. 2009). Note that the protocol parameters $\mathbf{V}$ of the decision variables are the MAC parameters $(\textit{macMinBE}, \textit{macMaxCSMABackoffs}, \textit{macMaxFrameRetries})$ of the standard. These expressions are a function of the busy probability α of CCA_1, the busy probability β of CCA_2, and the probability μ that a node attempts CCA_1. The expressions of μ, α, and β are derived by solving a system of non-linear equations numerically, see (Park et al. 2009) for further details.

In the following section, we derive the performance indicator of control systems which is a function of packet loss probability and delay induced by the wireless network.

3.3 Design of Estimator and Controller

In the previous section, we introduced an analytical model of the IEEE 802.15.4 MAC protocol for the packet loss probability and delay. In this section we briefly discuss the design of a feedback controller and present a control cost to analyze the control systems in Section 3.1. We first introduce our performance indicator as the quadratic cost function, which is an explicit function of the sampling period h, packet loss probability p, and delay τ of the network. Then, we design the estimator and controller under packet losses and delays. This is achieved by using results on optimal stochastic estimation and control under packet losses in (Schenato, Si-

nopoli, Franceschetti, Poola and Sastry 2007) and delays in (Nilsson 1998a).

3.4 Co-Design Framework

In this section, we discuss the co-design approach of a networked controlled system. We first propose the co-design approach which connects the analytical model of the wireless network described in Section 3.2 and the control design presented in Section 3.3. Then, we illustrate the proposed design approach through numerical examples.

3.4.1 Design Procedure

Fig. 9 shows the proposed design flow that each control loop of the network follows. The application designer provides the parameters of network setup Δ and the desired maximum quadratic cost of control systems J_{req}. Δ includes the important factors for modelling the wireless network such as a network topology, length of the packets, and the number of nodes. It is also possible that each control loop makes a different desired maximum quadratic cost J_{req}. Then, the control designer computes, off-line, an estimator and a state feedback according to (Schenato et al. 2007) and (Nilsson 1998a) for different packet loss probabilities and delays. Note that the control design process does not require any explicit considerations of the communication protocols or the network setup. Next, the network manager computes the achievable minimum quadratic cost of the networked control systems $J_{\min}$ according to the network model in Section 3.2 and the function of quadratic cost in Section 3.3. If the minimum quadratic cost $J_{\min}$ is less than the desired maximum quadratic cost J_{req}, then it is feasible. Note that any unrealistic desired control performance must be adapted by considering the feasibility. If the requirement of control performance is feasible, then the network manager computes the feasible set of sampling period, packet loss probability, and delay based on the network model. This is one of reasons that we develop the analytical modelling of the wireless network in the design process. The network model is an efficient tool since it reduces the computation complexity and development time compared to experience-based or simulation-based approaches, as in (Liu and Goldsmith 2004). Then, the network manager formulates and solves a constrained optimization problem, whereby the objective function is the energy consumption of the network and the constraints are the packet loss probability and delay, which are derived by the desired control performance J_{req}. More precisely,

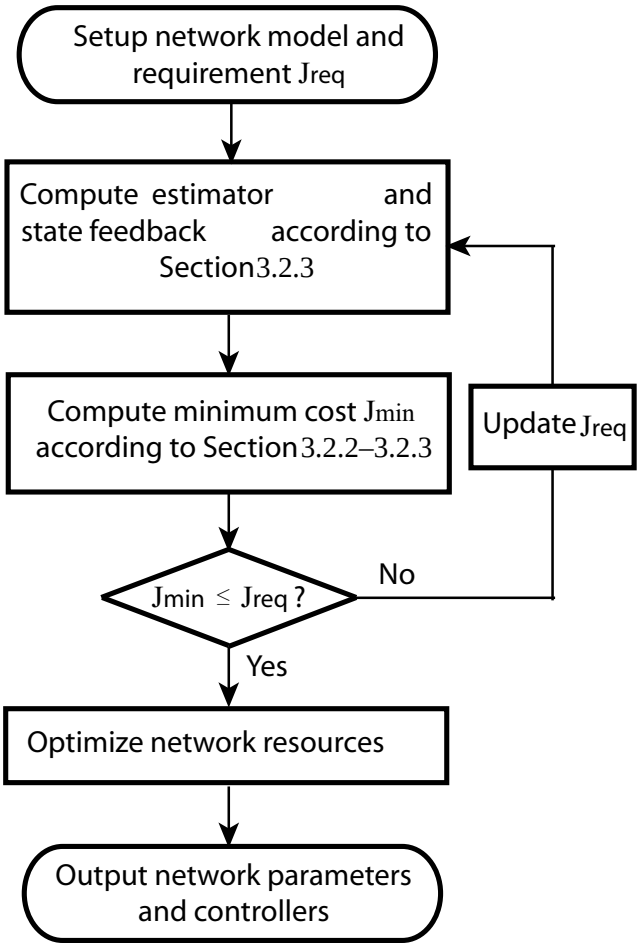

Figure 9: Flow diagram of co-design framework.

the constrained optimization problem in (24) is rewritten as follows

$$\min_{h,\mathbf{V}} \quad E_{\text{tot}}(h, \mathbf{V}, \Delta) \tag{25a}$$

$$\text{s.t.} \quad p(h, \mathbf{V}, \Delta) \leq p_{\text{req}}\,, \tag{25b}$$

$$\tau(h, \mathbf{V}, \Delta) \leq \tau_{\text{req}}\,. \tag{25c}$$

The decision variables are the sampling period h and the communication protocol parameters $\mathbf{V}$ depending on the network designer. Recall that the protocol parameters $\mathbf{V}$ are the MAC parameters (*macMinBE*, *macMaxCSMABackoffs*, *macMaxFrameRetries*) of the standard in this section. It is a challenging task to find the global optimal solution of the problem, since the derivation of exact analytical expressions is not possible due to the uncertainty of the wireless channel. One can find a sub-optimal solution using the steps described in the thesis (Park 2009). After solving the optimization problem, the network manager adapts the sampling period and the protocol parameters of the network. In addition, it sends the corresponding packet loss probability and delay of the network to the control designer. The control designer chooses the estimator and the state feedback based on the received information of the network.

In the following section, we illustrate our design strategy through numerical examples.

3.4.2 Illustrative Example

In this section, we show the achievable control performance by taking into account realistic simulation results. The quadratic cost is considered as a performance indicator of the control system. As an example we consider an unstable second-order plant in the form of (20) with

$$A = \begin{pmatrix} 3 & 1 \\ 0 & 1 \end{pmatrix},\ B = \begin{pmatrix} 0 \\ 1 \end{pmatrix},\ C = \begin{pmatrix} 1 & 0 \\ 0 & 1 \end{pmatrix},\ P_0 = 0.01I$$

$$W = I,\ U = 0.01,\ N = 0,\ R_w = I,\ R_v = 0.01I.$$

We observe the quadratic cost and the achievable region of control performance over different sampling periods, packet loss probabilities, and delays in Fig. 10. Fig. 10(a) shows the tradeoff between the quadratic cost, sampling period and packet loss probability when all packets have a fixed length. We assume that the packet delay is negligible ($\tau = 0$) to observe the pure effect of packet loss on the performance of the control systems. It is interesting to observe that as the

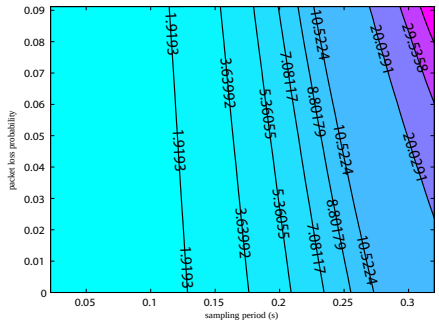

(a) Quadratic cost over different sampling periods and packet loss probabilities.

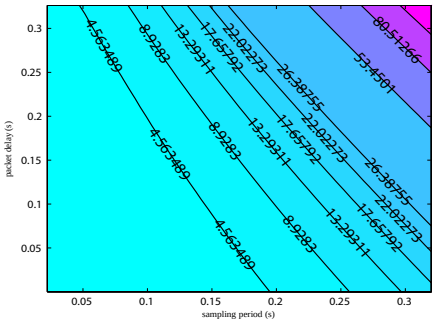

(b) Quadratic cost over different sampling periods and packet delays.

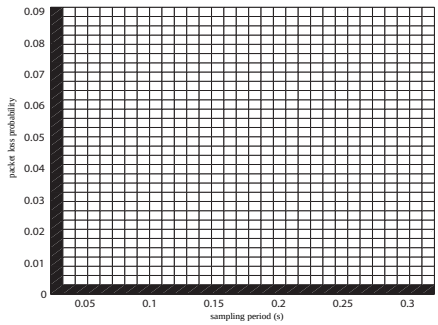

(c) Achievable region of the wireless network over different sampling periods with $M = 5$ nodes.

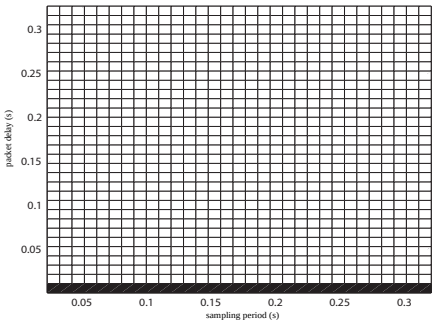

(d) Achievable region of the wireless network over different sampling periods with $M = 5$ nodes.

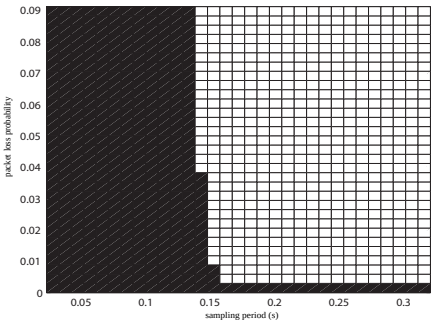

(e) Achievable region of the wireless network over different sampling periods with $M = 20$ nodes.

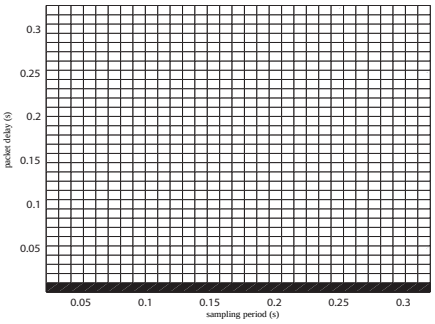

(f) Achievable region of the wireless network over different sampling periods with $M = 20$ nodes.

Figure 10: Quadratic cost and achievable region over different sampling periods, packet loss probabilities, and delays. To present the achievable region, we use a white square to denote that the wireless network meets a given packet loss probability and delay, and black squares otherwise.

sampling period increases, the quadratic cost is more sensitive with respect to the packet loss. In other words, packet losses at a higher sampling period are more critical than packet losses at a lower sampling period. Longer sampling periods increase the quadratic cost of control systems. Fig. 10(b) shows the quadratic cost with different sampling periods and packet delays for fixed packet lengths when there is no packet loss ($p = 0$). In a similar fashion, we derive the effects of packet delay on the quadratic cost.

Next, we show the achievable control performance by considering realistic simulation results of wireless networks. A point is achievable if it satisfies a given packet loss probability and delay for each sampling period. The achievable region is the set of all achievable points. Figs. 10(c) and 10(e) depict the achievable region with different sampling periods and packet loss probabilities for $M = 5$ and 20 nodes, respectively. In the figures, we use a white square to denote that the wireless network meets a given packet loss probability and delay, and black squares otherwise. Observe in Fig. 10(c) that the packet loss probability $p \leq 0.09$ is not achievable when the sampling period is very short $h \leq 0.03\,\text{s}$. Since very short sampling periods increase the traffic load of the network, then the packet loss probability is closer to the critical packet loss probability, above which the system is unstable. Hence, it is difficult to achieve a very low packet loss probability when the sampling period is very short. Observe that the area of the achievable region increases as the number of nodes decreases due to a lower packet collision probability. In a similar fashion, it is possible to analyze the effect of packet delay and sampling period in terms of achievable region. Notice that very short packet delays ($\tau < 0.01\,s$) are not achievable due to the default sensing and packet transmission time of the standard. Comparison of the achievable regions of Figs. 10(d) and 10(f) to 10(c) and 10(e) shows that the packet loss probability is more critical than the packet delay. The achievable quadratic cost of Fig. 10(a) is the achievable regions of the network marked by a white square in Figs. 10(c) and 10(e).

Fig. 11 shows the particular realization of the state response and control signal with different sampling periods $\bar{h} = 4.8\,\text{ms}$, $96\,\text{ms}$ and $M = 5$ nodes, 20 nodes. The initial condition is $\bar{x}_0 = [5\ 0]^T$ with covariance matrices $R_w = 0.01I$ and $R_v = 0.01I$. Note that the packet loss probability p and average delay $\bar{\tau}$ are computed by simulation results. In Fig. 11(a), we compare the first state response $x^{(1)}$ under the ideal case (no packet loss and no delay) with the state response under the realistic wireless network model of (Park et al. 2009) in order to investigate the effects of the wireless network. Observe that the step responses of the ideal case and the realistic wireless network model with $M = 20$ nodes and $\bar{h} = 96\,\text{ms}$ have a similar shape even though the settling time of the realistic wireless net-

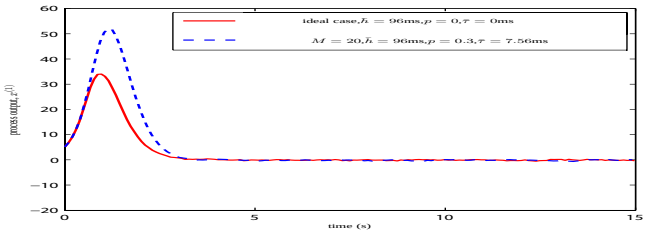

(a) process output of ideal case and the realistic wireless network model with $\bar{h} = 96$ ms and $M = 20$ nodes.

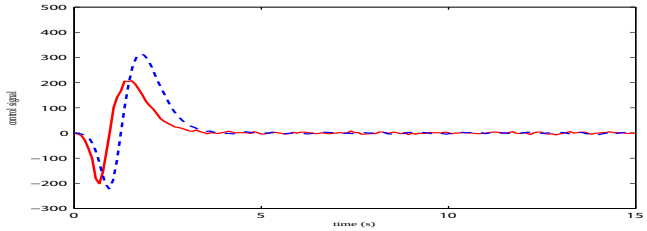

(b) control signal of ideal case and the realistic wireless network model with $\bar{h} = 96$ ms and $M = 20$ nodes.

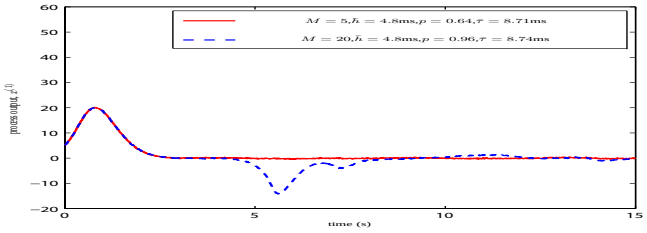

(c) process output of the realistic wireless network model with $\bar{h} = 4.8$ ms and $M = 5, 20$ nodes.

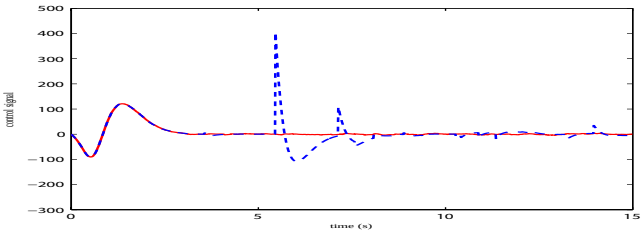

(d) control signal of the realistic wireless network model with $\bar{h} = 4.8$ ms and $M = 5, 20$ nodes.

Figure 11: State response and control signal of the ideal case (no packet loss and no delay) and the realistic wireless network model with the initial condition $[5\ \ 0]^T$, covariance matrices $R_w = 0.01I$ and $R_v = 0.01I$, different sampling periods $\bar{h} = 4.8, 96$ ms and $M = 5, 20$ nodes. The particular realization is shown out of $M = 5, 20$ nodes.

work model with $M = 20$ nodes is longer due to packet loss $p = 0.3$ and mean delay $\bar{\tau} = 7.56$ ms. However, Fig. 11(c) shows that reducing the sampling period $\bar{h} = 4.8$ ms does not improve the step response with $M = 20$ nodes, because of the higher packet loss probability $p = 0.96$ and the higher mean delay $\bar{\tau} = 8.74$ ms. Note that both packet loss and mean delay increase when the sampling period decreases i.e., heavy network traffic load. The realistic wireless network model with $M = 5$ nodes and $\bar{h} = 4.8$ ms gives the best step response in Fig. 11(c). This behavior comes from the fact that the packet collision probability is smaller for $M = 5$ than $M = 20$. Naturally, this shows that the optimal sampling period of a wireless networked control system is a challenging problem which requires a proper abstraction of the wireless network.

Fig. 12 shows the quadratic cost of a control system and throughput of the wireless network over different sampling periods. The throughput is the average rate of successful data transmission over a communication channel. In the figure, "J_∞^{i}" and "J_∞^{r}" refer to the cost bound $J_\infty^{\max}$ of the infinite horizon quadratic cost with the ideal case and the realistic model in (Park et al. 2009), respectively. Recall that J_N^* is the finite horizon quadratic cost, which is computed by the measured packet loss probability and the delay from realistic simulations. Observe that the finite horizon cost J_N^* follows the cost bound of infinite horizon cost J_∞^{r} based on the realistic model of the wireless network. Notice that the cost J_N^* of shorter sampling periods is larger than the cost bound J_∞^{r} due to the higher packet loss probability and the mean value approximation described in Section 3.3. Observe that the control performance when using an ideal network increases monotonically as the sampling period increases. However, when using a real network, a shorter sampling period does not minimize the quadratic cost of the control systems, because of the higher packet loss probability when the traffic load is high. In other words, the packet loss is a more critical factor compared to the delay as the sampling period decreases. When the sampling period is very short, then a control system goes unstable due to the high packet loss probability. In addition, the two curves of the cost J_∞^{i} and J_∞^{r} coincide for longer sampling periods. This is because the packet loss probability is negligible for large sampling periods due to the lower traffic load on the network. Hence, when the sampling period is larger, the sampling period is the dominant factor in the quadratic cost compared to the packet loss probability and delay. When we flip the curve of throughput on the Y-axis, it is possible to observe a similar trend of behavior with the curve of quadratic cost. Note that the closer the throughput is to 1, the better the utility of the wireless network. As the sampling period $h < 0.13$ s increases, the quadratic cost decreases and the throughput increases. For a longer sampling pe-

riod $h > 0.15$, the performance of both the control and the communication system degrades as the sampling period increases. In our example, the optimal sampling period that minimizes the quadratic cost of the control system is close to the one that maximizes the throughput of the network.

Let us consider a desired maximum quadratic cost J_{req} greater than the minimum value of the quadratic cost. Then, we have two feasible sampling periods $\mathcal{S}$ and $\mathcal{L}$ in Fig. 12. However, the performance of the wireless network is still heavily affected by the choice of the sampling period of $\mathcal{S}$ and $\mathcal{L}$ due to different traffic loads, as we discussed earlier. Note that choosing the shorter sampling period $\mathcal{S}$ would obviously lead to a higher packet loss probability and delay than choosing the longer sampling period $\mathcal{L}$. Furthermore, the longer sampling period $\mathcal{L}$ leads to lower network energy consumption than the shorter sampling period $\mathcal{S}$ (see details in (Park et al. 2009, Pollin, Ergen, Ergen, Bougard, Perre, Moerman, Bahai, Varaiya and Catthoor 2008)). Recall that the energy efficiency is one of critical issue for sensor nodes due to limited battery power. This motivates our co-design approach of networked control systems running over WSNs. From these simulation results, we conclude that it is important to design the parameters of control system and communication network jointly.

3.4.3 Conclusion

We addressed the problem of joint design of multiple control systems over the wireless network imposed by the IEEE 802.15.4 standard. We propose a co-design approach by considering the critical aspects for both control and communication systems. In particular, the constrained optimization problem is formulated, where the objective function is the energy consumption of the network and the constraints are the packet loss probability and delay, which are derived from the desired control performance. We use the quadratic cost as a performance indicator, which is an explicit function of the sampling period, packet loss probability, and delay of the network. The analytical model of the IEEE 802.15.4 standard is used to connect the control and communication systems. Simulation results of the packet loss and delay using the IEEE 802.15.4 standard show that the achievable performance of the control system running over the wireless network. We illustrate the efficiency of the co-design approach through numerical examples.

Event-based control is a promising alternative to conventional periodic control, especially for systems with limited computation capabilities and communication capacities. Future investigations include the extension of the aforementioned work to the event-based controller.

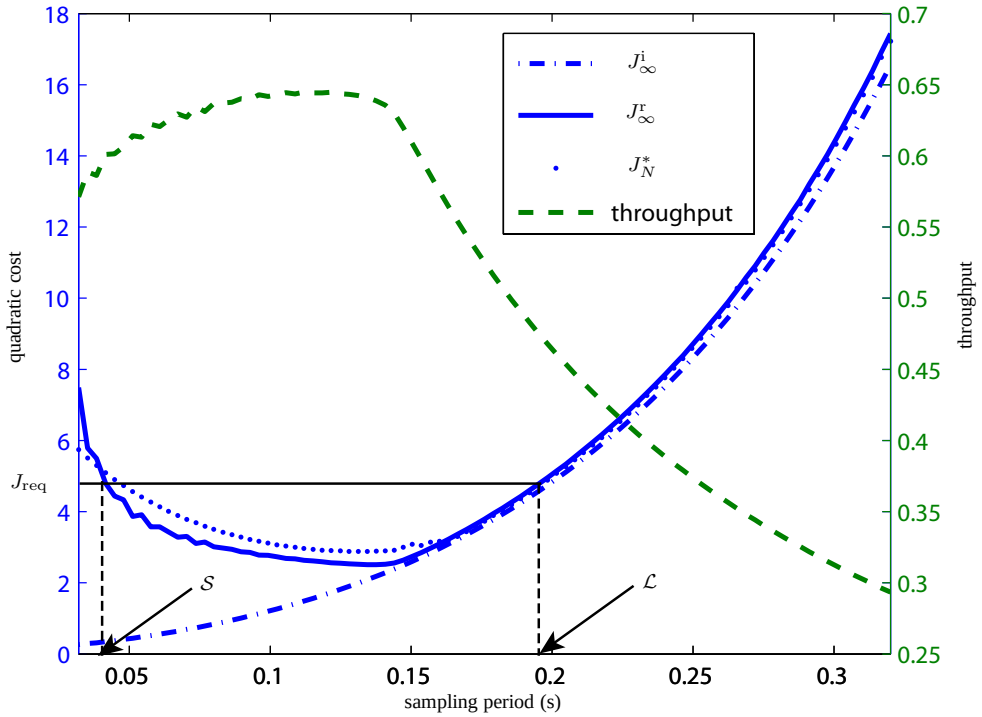

Figure 12: Quadratic cost of control system and throughput of the wireless network over different sampling periods. "J_∞^{i}" and "J_∞^{r}" refer to the cost bound $J_\infty^{\max}$ of the infinite horizon quadratic cost with ideal case and realistic model in (Park et al. 2009), respectively. "J_N^*" denotes the finite horizon quadratic cost which is computed by the measured packet loss probability and delay of the simulation.

4 Cooperative data detection using a CDMA protocol

In this section, we consider the exchange of information between nodes grouped in two clusters. The data are transmitted over multiple access fading channels. Data are recovered in a totally blind way.

Multiple access protocols such as Time Division Multiple Access (TDMA) can induce a latency that can be damaging for control purposes for example. In this case, Direct-Sequence Code Division Multiple Access (DS-CDMA) is certainly well indicated. In the last decade, by exploiting several diversities, new signal processing techniques based on tensor modeling have been developed. With a very high efficiency, they allow the blind estimation of transmitted information sequences (Sidiropoulos, Giannakis and Bro 2000, de Almeida, Favier and Mota 2007, Nion and De Lathauwer 2008, Kibangou and Favier 2009). In general, these works are devoted to communication systems with an antenna array at the receiver. However, many wireless devices are limited by size, hardware complexity or other constraints to a single antenna. The powerful tensor based methods cannot be applied for such nodes. By resorting to the idea of collaborative signal processing, we show how estimating the channel, symbols, and codes in a distributed way when each node in the network has a single antenna. The received data samples can be stored in a three-way array, or a third-order tensor, admitting a PARAFAC model. In general, the parameters of the PARAFAC model are estimated using an Alternating Least Squares (ALS) algorithm. We derive a distributed version of ALS using average consensus iterations. Average consensus is an important problem in algorithm design for distributed computing. In its distributed framework, it has been extensively studied in computer science (distributed agreement and synchronization problems for example). It is is a central topic for load balancing (with divisible tasks) in parallel computers and also has found application in distributed coordination of mobile autonomous agents, distributed data fusion in sensor networks, and distributed estimation and control (Xiao, Boyd and Kim 2007).

In the sequel, we will make use the properties of the Khatri-Rao product and

the Frobenius norm given below:

$$vec(\mathbf{X}diag(\mathbf{z})\mathbf{Y}^T) = (\mathbf{Y} \odot \mathbf{X})\mathbf{z}, \quad (26)$$

$$\mathbf{X} \odot \mathbf{Y} = \mathbf{\Pi}(\mathbf{Y} \odot \mathbf{X}), \quad (27)$$

$$\|\mathbf{X}\|_F^2 = \|\mathbf{\Pi}\mathbf{X}\|_F^2, \quad (28)$$

$$\left\| \begin{pmatrix} \mathbf{X}_1 & \cdots & \mathbf{X}_M \end{pmatrix} \right\|_F^2 = \sum_{m=1}^{M} \|\mathbf{X}_m\|_F^2, \quad (29)$$

$$\left\| \begin{pmatrix} \mathbf{x}_1 & \cdots & \mathbf{x}_M \end{pmatrix} \right\|_F^2 = \sum_{m=1}^{M} \|\mathbf{x}_m\|_2^2, \quad (30)$$

$\mathbf{\Pi}$, a permutation matrix, and $\mathbf{X}$ being matrices with compatible dimensions.

4.1 Problem Statement

Let us consider nodes grouped in two clusters A and B, where the Q nodes in cluster A transmit their information to the K nodes in cluster B using a synchronous DS-CDMA protocol through a flat fading channel. Each of the nodes spreads its information sequence $s_{n,q}$, $n = 1, \cdots, N$, and encodes it using a code $\{c_{p,q}\}$ of length P before transmission through an unknown channel characterized by a fading gain $a_{k,q}$, for a transmission between the qth sensor of cluster A and the kth sensor of cluster B. The baseband received signal of each node is sampled at the chip rate and decomposed into its polyphase components. So, in the noiseless case, the signal received by the kth node of cluster B, for the nth symbol and the pth chip is given by:

$$x_{k,p,n} = \sum_{q=1}^{Q} a_{k,q} c_{p,q} s_{n,q}. \quad (31)$$

If a central node collects the received signal samples $x_{k,p,n}$, we can build a third-order tensor $\mathbb{X} \in \mathbb{C}^{K \times P \times N}$ from these samples. The data collected from a given node k can be cast into a $P \times N$ matrix

$$\mathbf{X}_{k..} = \begin{pmatrix} x_{k,1,1} & \cdots & x_{k,1,N} \\ \vdots & \ddots & \vdots \\ x_{k,P,1} & \cdots & x_{k,P,N} \end{pmatrix} = \mathbf{C}diag(\mathbf{A}_{k.})\mathbf{S}^T \quad (32)$$

that can be viewed as a slice of $\mathbb{X}$, where $\mathbf{A} = [a_{k,q}] \in \mathbb{C}^{K \times Q}$, $\mathbf{C} = [c_{p,q}] \in \mathbb{C}^{P \times Q}$, and $\mathbf{S} = [s_{n,q}] \in \mathbb{C}^{N \times Q}$. In order to recover the information symbols $s_{n,q}$ solely

from $\mathbb{X} \in \mathbb{C}^{K\times P\times N}$, we can then make use of tensor-based signal processing methods developed in the last decade (Sidiropoulos et al. 2000).

From (31), one can note that $\mathbb{X}$ admits a PARAFAC model, in which the tensor is completely characterized by the three loading, or factor, matrices $\mathbf{A}$, $\mathbf{C}$, and $\mathbf{S}$. According to the Kruskal's condition the factor matrices are essentially unique if (Kruskal 1977, Sidiropoulos et al. 2000)

$$k_{\mathbf{A}} + k_{\mathbf{C}} + k_{\mathbf{S}} \geq 2(Q+1). \tag{33}$$

The three vertically unfolded matrix representations for $\mathbb{X}$ are respectively given by:

$$\mathbf{X}_1 = (\mathbf{A} \odot \mathbf{C})\,\mathbf{S}^T \in \mathbb{C}^{KP\times N},\ \ \mathbf{X}_2 = (\mathbf{C} \odot \mathbf{S})\,\mathbf{A}^T \in \mathbb{C}^{PN\times K},$$

$$\mathbf{X}_3 = (\mathbf{S} \odot \mathbf{A})\,\mathbf{C}^T \in \mathbb{C}^{NK\times P}.$$

Given the tensor $\mathbb{X}$, the factor matrices $\mathbf{A}$, $\mathbf{C}$, and $\mathbf{S}$ can be estimated by alternately minimizing the cost functions in the LS sense

$$\mathcal{J}_1 = \left\|\mathbf{X}_1 - (\mathbf{A} \odot \mathbf{C})\,\mathbf{S}^T\right\|_F^2, \tag{34}$$

$$\mathcal{J}_2 = \left\|\mathbf{X}_2 - (\mathbf{C} \odot \mathbf{S})\,\mathbf{A}^T\right\|_F^2, \tag{35}$$

$$\mathcal{J}_3 = \left\|\mathbf{X}_3 - (\mathbf{S} \odot \mathbf{A})\,\mathbf{C}^T\right\|_F^2. \tag{36}$$

given initial approximations of two factor matrices, $\mathbf{A}^{(0)}$ and $\mathbf{C}^{(0)}$ for instance.

As stated above, the kth node in cluster B receives data that can be cast in the matrix $\mathbf{X}_{k..}$. In order, to retrieve the informative symbol matrix $\mathbf{S}$, a bilinear decomposition is involved. Such a decomposition is generally non unique. Uniqueness of PARAFAC (a trilinear decomposition) can be exploited by sending the matrices $\mathbf{X}_{k..}$ to a central node where collected data can be cast into a tensor $\mathbb{X}$. The central node performs the PARAFAC decomposition of $\mathbb{X}$ and then send the estimated factor matrices, or at least $\mathbf{S}$ to the sensors. Due to the existence of a central node, such a scheme is particularly vulnerable. Resorting to distributed estimation is then well suited. One can imagine that the nodes exchange their received data samples with their neighbors. As a consequence, after such an information exchange, from its own data matrix and those received from its neighbors, each node can form a tensor, which is in fact a sub-tensor of $\mathbb{X}$. Unfortunately, we cannot ensure that all sub-tensors inherit the uniqueness property of the global tensor. Therefore, in such a scheme, some node can obtain undesirable estimates,

i.e. estimates that cannot be linked to the actual factor matrices in a unique way. The purpose of the following section is to derive a distributed estimation scheme, preserving the PARAFAC uniqueness property.

4.2 Distributed ALS Algorithm

Recently, a great effort has been devoted to the derivation of distributed estimation algorithms (Xiao et al. 2007, Mateos, Schizas and Giannakis 2007, Bolognani, Del Favero, Schenato and Varagnolo 2008). Most of them make use of the consensus algorithm. In this framework, from the centralized ALS, in (Kibangou and de Almeida 2010) we have derived a distributed ALS algorithm (D-ALS).

4.2.1 Consensus based estimation of the symbol matrix S

The symbol matrix $\mathbf{S}$ can be estimated by minimizing the cost function $\mathcal{J}_1$, which can be rewritten as:

$$\mathcal{J}_1 = \left\| \mathbf{X}_1 - \mathbf{Y}\mathbf{S}^T \right\|_F^2,$$

with $\mathbf{Y} = \mathbf{A} \odot \mathbf{C}$. From the definition of the Khatri-Rao product, we get:

$$\mathbf{Y} = \begin{pmatrix} \mathbf{Y}_1 \\ \vdots \\ \mathbf{Y}_K \end{pmatrix} = \begin{pmatrix} \mathbf{C}diag(\mathbf{A}_{1.}) \\ \vdots \\ \mathbf{C}diag(\mathbf{A}_{K.}) \end{pmatrix}.$$

By minimizing $\mathcal{J}_1$, given $\mathbf{Y}$, we get

$$\hat{\mathbf{S}}^T = \left(\mathbf{Y}^H\mathbf{Y}\right)^{-1}\mathbf{Y}^H\mathbf{X}_1.$$

This solution can also be written as:

$$\hat{\mathbf{S}}^T = \left(\frac{1}{K}\sum_{k=1}^{K}\mathbf{Y}_k^H\mathbf{Y}_k\right)^{-1}\left(\frac{1}{K}\sum_{k=1}^{K}\mathbf{Y}_k^H\mathbf{X}_{k..}\right). \tag{37}$$

Note that the computation of (37) results on averaging local estimates $\mathbf{\Gamma}_k(0) = \mathbf{Y}_k^H\mathbf{Y}_k$ and $\mathbf{\Theta}_k(0) = \mathbf{Y}_k^H\mathbf{X}_{k..}$. Such averaging can be achieved using the consensus algorithm. We have to run two average consensus in parallel so that

$$\mathbf{\Gamma}_k(t) \rightarrow \frac{1}{K}\sum_{k=1}^{K}\mathbf{\Gamma}_k(0) = \frac{1}{K}\sum_{k=1}^{K}\mathbf{Y}_k^H\mathbf{Y}_k,$$

$$\boldsymbol{\Theta}_k(t) \rightarrow \frac{1}{K}\sum_{k=1}^{K}\boldsymbol{\Theta}_k(0) = \frac{1}{K}\sum_{k=1}^{K}\mathbf{Y}_k^H\mathbf{X}_{k..}.$$

Therefore, the local estimate of $\mathbf{S}^T$, defined as $\hat{\mathbf{S}}_k^T = \boldsymbol{\Gamma}_k^{-1}(t)\boldsymbol{\Theta}_k(t)$ converges towards $\hat{\mathbf{S}}^T$. One can note that for the calculation of $\boldsymbol{\Gamma}_k(0)$ and $\boldsymbol{\Theta}_k(0)$ all the sensors should have the same approximation of the loading matrix $\mathbf{C}$, a non restrictive condition.

4.2.2 Consensus based estimation of the code matrix $\mathbf{C}$

The code matrix $\mathbf{C}$ can be estimated by minimizing $\mathcal{J}_3$, which can be rewritten as $\mathcal{J}_3 = \left\|\mathbf{X}_3 - \tilde{\mathbf{Z}}\mathbf{C}^T\right\|_F^2$, with $\tilde{\mathbf{Z}} = (\mathbf{S} \odot \mathbf{A})$. By using the property (28) of the Frobenius norm, we also have $\mathcal{J}_3 = \left\|\boldsymbol{\Pi}\mathbf{X}_3 - \mathbf{Z}\mathbf{C}^T\right\|_F^2$ where

$$\mathbf{Z} = \mathbf{A} \odot \mathbf{S} = \boldsymbol{\Pi}\tilde{\mathbf{Z}} = \begin{pmatrix} \mathbf{Z}_1 \\ \mathbf{Z}_2 \\ \vdots \\ \mathbf{Z}_K \end{pmatrix},$$

with $\mathbf{Z}_k = \mathbf{S}diag(\mathbf{A}_{k.})$. Therefore, the minimization of $\mathcal{J}_3$ yields

$$\hat{\mathbf{C}}^T = \left(\mathbf{Z}^H\mathbf{Z}\right)^{-1}\mathbf{Z}^H\boldsymbol{\Pi}\mathbf{X}_3.$$

This solution can also be written as:

$$\hat{\mathbf{C}}^T = \left(\frac{1}{K}\sum_{k=1}^{K}\mathbf{Z}_k^H\mathbf{Z}_k\right)^{-1}\left(\frac{1}{K}\sum_{k=1}^{K}\mathbf{Z}_k^H\mathbf{X}_{k..}^T\right). \tag{38}$$

As previously, the computation of (38) results on averaging local estimates $\boldsymbol{\Lambda}_k(0) = \mathbf{Z}_k^H\mathbf{Z}_k$ and $\boldsymbol{\Psi}_k(0) = \mathbf{Z}_k^H\mathbf{X}_{k..}^T$. The averaging process by means of the consensus algorithm yields:

$$\boldsymbol{\Lambda}_k(t) \rightarrow \frac{1}{K}\sum_{k=1}^{K}\boldsymbol{\Lambda}_k(0) = \frac{1}{K}\sum_{k=1}^{K}\mathbf{Z}_k^H\mathbf{Z}_k,$$

$$\boldsymbol{\Psi}_k(t) \rightarrow \frac{1}{K}\sum_{k=1}^{K}\boldsymbol{\Psi}_k(0) = \frac{1}{K}\sum_{k=1}^{K}\mathbf{Z}_k^H\mathbf{X}_{k..}^T.$$

Therefore, the local estimate of $\mathbf{C}^T$, defined as $\hat{\mathbf{C}}_k^T = \boldsymbol{\Lambda}_k^{-1}(t)\boldsymbol{\Psi}_k(t)$ converges towards $\hat{\mathbf{C}}^T$.

4.2.3 Estimation of the channel matrix A

The channel parameters are intrinsically local. Therefore there is no need to share these parameters between different sensors. In a centralized scheme, the channel matrix is obtained by minimizing $\mathcal{J}_2$. Knowing that the three cost functions are equivalent, we derive the estimation of the channel parameter by minimizing $\mathcal{J}_1$. We can note that by using (29) and (30), $\mathcal{J}_1$ can also be written as

$$\begin{aligned}
\mathcal{J}_1 &= \left\|\mathbf{X}_1^T - \mathbf{S}(\mathbf{A}\odot\mathbf{C})^T\right\|_F^2 \\
&= \left\|\left(\mathbf{X}_{1..}^T - \mathbf{S}diag(\mathbf{A}_{1.})\mathbf{C}^T \cdots \mathbf{X}_{K..}^T - \mathbf{S}diag(\mathbf{A}_{K.})\mathbf{C}^T\right)\right\|_F^2 \\
&= \sum_{k=1}^{K}\left\|\mathbf{X}_{k..}^T - \mathbf{S}diag(\mathbf{A}_{k.})\mathbf{C}^T\right\|_F^2 \\
&= \sum_{k=1}^{K}\left\|vec(\mathbf{X}_{k..}^T) - (\mathbf{C}\odot\mathbf{S})\,\mathbf{A}_{k.}^T\right\|_2^2. \qquad (39)
\end{aligned}$$

As a consequence, by the code and the symbol matrices by their local estimates, the local channel parameters can be estimated as follows:

$$\hat{\mathbf{A}}_{k.}^T = (\hat{\mathbf{C}}_k \odot \hat{\mathbf{S}}_k)^{\dagger} vec(\mathbf{X}_{k..}^T). \qquad (40)$$

4.2.4 Average consensus algorithm

Let $\mathcal{G} = \{\mathcal{K}, \mathcal{E}\}$ be an undirected connected graph representing the communication graph between the collaborating nodes. $\mathcal{K} = \{1, \cdots, K\}$ and $\mathcal{E}$ denote respectively the node set and the edge set, where each edge $\{i, j\} \in \mathcal{E}$ is an unordered pair of distinct nodes. Let $\mathbf{R}_k(0)$ be a matrix assigned to node k at time $t = 0$. The distributed average consensus problem consists in computing the average $(1/K)\sum_{k=1}^{K}\mathbf{R}_k(0)$ at every node, via local communication and computation on the graph. So, node k carries out its update, at each step, based on its local state and communication with its neighbors $\mathcal{K}_i = \{j|\{i, j\} \in \mathcal{E}\}$.

There are several simple methods for distributed average consensus. For example, each node can store a table of all initial node values known at that time. At each step each pair of neighbors exchange tables of initial values and update their tables. In this flooding algorithm, all nodes know all initial values in a number of steps equal to the diameter of the graph, at which point each can compute the average (Xiao et al. 2007). In widely used average consensus algorithms, each

node updates itself by adding a weighted sum of differences between neighboring node values and its own. In matrix form, we get:

$$\mathbf{R}_k(t+1) = \mathbf{R}_k(t) + \sum_{j \in \mathcal{K}_i} w_{k,j} \left(\mathbf{R}_j(t) - \mathbf{R}_k(t) \right), \tag{41}$$

where $w_{k,j}$ is a weight associated with the edge $\{k, j\}$. In the sequel, we assume that the weights are symmetric. Asymptotic convergence is achieved by choosing for example uniform weights

$$w_{k,j} = 1/d_k \quad j \neq k, \{k, j\} \in \mathcal{E}, \tag{42}$$

where d_i is the degree of node i.

4.2.5 Distributed ALS algorithm using average consensus

The D-ALS algorithm is constituted by interlacing local ALS steps with consensus iterations. By considering perfect exchange during consensus iterations, it is summarized below:

1. For $k = 1, \cdots, K$, initialize $\hat{\mathbf{C}}_k(0) = \mathbf{\Omega} \in \mathbb{C}^{P \times Q}$, with $\mathbf{\Omega}$ chosen in a pre-definite set of possible code matrices, and $\hat{\mathbf{A}}_{k.}(0) \in \mathbb{C}^{1 \times Q}$ with random values. Set the D-ALS iteration $i = 0$, and select a number T of consensus iterations.

2. For $k = 1, \cdots, K$, compute $\mathbf{Y}_k(i) = \hat{\mathbf{C}}_k(i) diag(\hat{\mathbf{A}}_{k.}(i))$, $\mathbf{\Gamma}_k(i, 0) = \mathbf{Y}_k^H(i)\mathbf{Y}_k(i)$, and $\mathbf{\Theta}_k(i, 0) = \mathbf{Y}_k^H(i)\mathbf{X}_{k..}$.

3. Run the consensus algorithm for $\mathbf{\Gamma}_k$ and $\mathbf{\Omega}_k$

   (a) For $t = 0, 1, \cdots, T-1$,

   $$\mathbf{\Gamma}_k(i, t+1) = \mathbf{\Gamma}_k(i, t) + \sum_{j \in \mathcal{K}_k} w_{k,j} \left(\mathbf{\Gamma}_j(i, t) - \mathbf{\Gamma}_k(i, t) \right)$$

   $$\mathbf{\Theta}_k(i, t+1) = \mathbf{\Theta}_k(i, t) + \sum_{j \in \mathcal{K}_k} w_{k,j} \left(\mathbf{\Theta}_j(i, t) - \mathbf{\Theta}_k(i, t) \right).$$

   (b) Set $\mathbf{\Gamma}_k(i) = \mathbf{\Gamma}_k(i, T)$ and $\mathbf{\Omega}_k(i) = \mathbf{\Omega}_k(i, T)$.

4. Increment i.

5. Compute the local estimates of the symbol matrix $\mathbf{S}$

$$\hat{\mathbf{S}}_k(i) = \mathbf{\Gamma}_k^{-1}(i-1)\mathbf{\Omega}_k(i-1).$$

6. For $k = 1, \cdots, K$, compute $\mathbf{Z}_k(i) = \hat{\mathbf{S}}_k(i) diag(\hat{\mathbf{A}}_{k\cdot}(i-1))$, $\mathbf{\Lambda}_k(i,0) = \mathbf{Z}_k^H(i)\mathbf{Z}_k(i)$, and $\mathbf{\Psi}_k(i,0) = \mathbf{Z}_k^H(i)\mathbf{X}_{k\cdot\cdot}^T$.

7. Run the consensus algorithm for $\mathbf{\Lambda}_k$ and $\mathbf{\Psi}_k$

   (a) For $t = 0, 1, \cdots, T-1$,

$$\mathbf{\Lambda}_k(i,t+1) = \mathbf{\Lambda}_k(i,t) + \sum_{j \in \mathcal{K}_k} w_{k,j} \left(\mathbf{\Lambda}_j(i,t) - \mathbf{\Lambda}_k(i,t)\right)$$

$$\mathbf{\Psi}_k(i,t+1) = \mathbf{\Psi}_k(i,t) + \sum_{j \in \mathcal{K}_k} w_{k,j} \left(\mathbf{\Psi}_j(i,t) - \mathbf{\Psi}_k(i,t)\right).$$

   (b) Set $\mathbf{\Lambda}_k(i) = \mathbf{\Lambda}_k(i,T)$ and $\mathbf{\Psi}_k(i) = \mathbf{\Psi}_k(i,T)$.

8. Compute the local estimates of the code matrix $\mathbf{C}$

$$\hat{\mathbf{C}}_k(i) = \mathbf{\Lambda}_k^{-1}(i)\mathbf{\Psi}_k(i).$$

9. Compute the local estimates of the channel parameters

$$\hat{\mathbf{A}}_{k\cdot}^T(i) = \left(\hat{\mathbf{C}}_k(i) \odot \hat{\mathbf{S}}_k(i)\right)^{\dagger} vec(\mathbf{X}_{k\cdot\cdot}^T)$$

10. Return to step 2 until a convergence criterion is reached.

4.3 Simulation Results

In this section, we present some results obtained by simulating a network with $Q = 3, 4$ and $K = 9$. The informative symbols were randomly generated from a QPSK alphabet. The code sequences were orthogonal binary sequences taking values from $\{-1, 1\}$. We considered three scenarios for the connection topology between the sensors in cluster B: a ring (all the sensors have a connectivity degree equals to 3), a grid (the connectivity degree are: $4, 6, 4, 6, 9, 6, 4, 6, 4$), and a modified grid $(3, 6, 4, 6, 7, 6, 4, 6, 4)$. We varied the number of consensus iterations between 1 and 3. We denoted by D-ALS(i,j), the D-ALS corresponding to the ith topology of connection with j consensus iterations. For

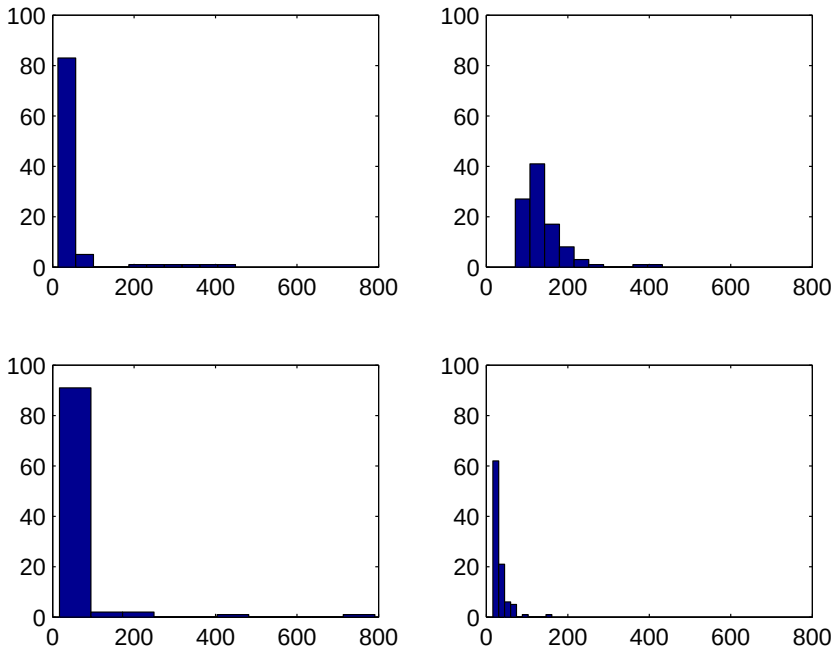

Figure 13: Histogram of the number of iterations for convergence in the ALS (top left) and D-ALS cases: ring (top right), grid (bottom left), modified grid (bottom right).

the average consensus iterations, the weights were computed using the uniform scheme (Blondel, Hendrickx, Olshevsky and Tsitsiklis 2005). The results below are averaged values over 100 independent Monte-Carlo runs. The performance is evaluated according to the NMSE (Normalized Mean Square Error), given by: $(1/K)\sum_{k=1}^{K}\frac{\left\|\mathbf{X}_{k..}-\hat{\mathbf{C}}_k diag(\hat{\mathbf{A}}_k)\hat{\mathbf{S}}_k^T\right\|_F^2}{\|\mathbf{X}_{k..}\|_F^2}$. We considered 1000 iterations of ALS. For both ALS and D-ALS, the convergence rate were greater than 90%. In Fig. 13, we depict the histogram corresponding to the number of iterations required for the algorithm convergence. We can note that the behavior of the ALS and D-ALS approaches are similar except for the case where the topology of connection in cluster B corresponds to a ring (We used three consensus iterations).

In Figures 14 and 15, the NMSE (mean and median values) is plotted as a

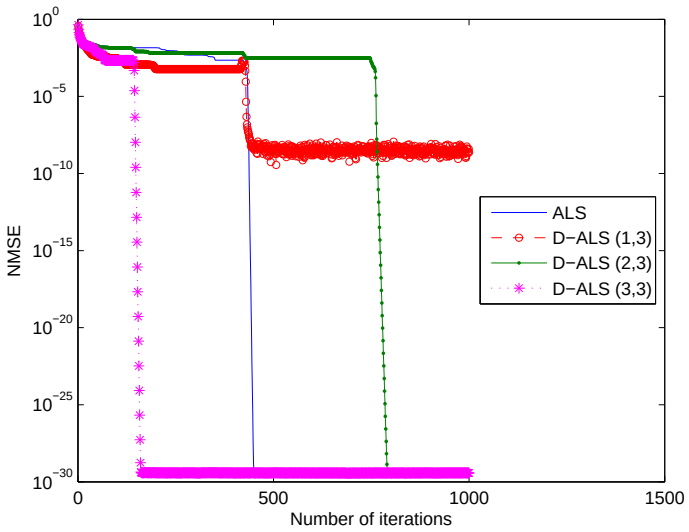

Figure 14: Mean NMSE for $Q = 3$ and three consensus iterations.

function of the number of iterations. It can be seen that the connection topology impacts the convergence of the D-ALS algorithm. Connection topologies with greater connectivity degree have convergence properties (speed and final value) similar to those obtained with ALS.

In Fig. 16, we note that even for a single consensus iteration the D-ALS algorithm converges towards the same value than ALS. However, the convergence speed is lower. It can be accelerated by increasing the number of consensus iterations.

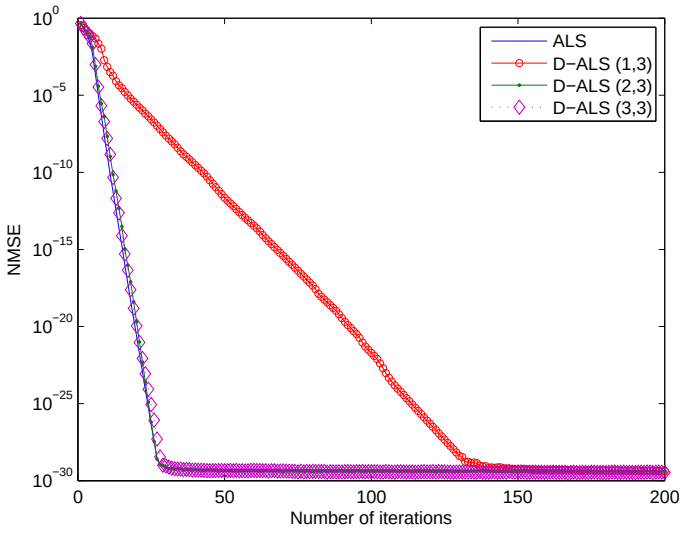

Figure 15: Median NMSE for $Q = 3$ and three consensus iterations.

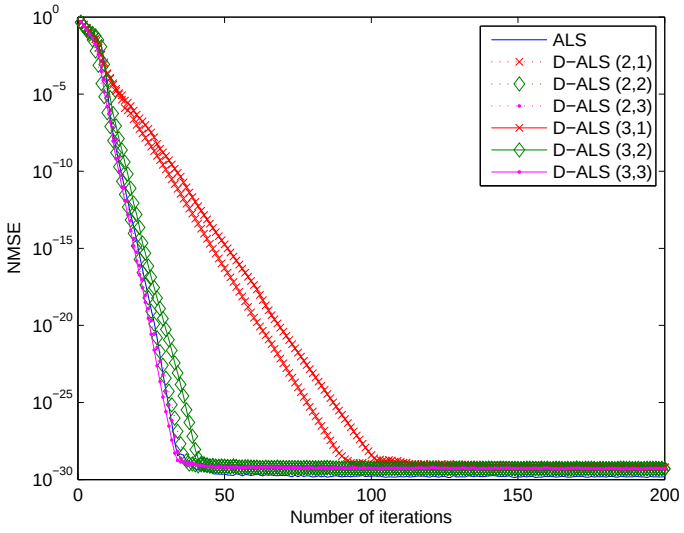

Figure 16: Median NMSE for $Q = 4$ and different number of consensus iterations.

5 Conclusions

For Task 3.4 we have considered five problems in the scope of network protocols for control applications. Several joint design approaches have been developed and studied.

- We propose a new method to optimize the allocation of communication rates in control over noisy channels. The overall objective function is derived based on the high-rate approximation theory and the constrained optimization problem is solved by means of Lagrangian duality theory. It is shown that non-uniform quantization is in general the best strategy for feedback control over noisy channels. It is also shown that the proposed method has better performance when compared to arbitrarily selected rate allocations.

- We have addressed the problem of joint design of multiple control systems over the wireless network imposed by the IEEE 802.15.4 standard. We propose a co-design approach by considering the critical aspects of both control and communication systems. A constrained optimization problem is formulated, where the objective function is the energy consumption of the network and the constraints are the packet loss probability and delay. Also, the analytical model of the IEEE 802.15.4 standard is used to connect the control and communication systems. Numerical simulation is conducted to illustrate the efficiency of the co-design approach and the achievable performance of the control system running over the wireless network.

- We have studied cooperative data detection using a CDMA protocol for exchange of information between nodes grouped in two clusters. We derive a distributed version of ALS algorithm using average consensus iterations. Numerical comparison between ALS and distributed ALS is carried out. It is shown that the behavior of the two approaches are similar except some special cases. It is also shown that the connection topology impacts the convergence of the distributed ALS algorithm.

References

Aström, K. J. and Wittenmark, B.: 1997, *Computer-Controlled Systems*, Prentice Hall.

Bao, L., Skoglund, M., Fischione, C. and Johansson, K. H.: 2010, Rate allocation with power constraints for quantized control over noisy channels, *IEEE Transactions on Signal Processing* . submitted.

Blondel, V., Hendrickx, J., Olshevsky, A. and Tsitsiklis, J.: 2005, Convergence in multiagent coordination, consensus, and flocking, *Proc. of the joint 44th IEEE Conf. on Decision and Control (CDC) and European Control Conf (ECC)*, Seville, Spain, pp. 2996–3000.

Bolognani, S., Del Favero, S., Schenato, L. and Varagnolo, D.: 2008, Distributed sensor calibration and least-square parameter identification in WSNs using consensus algorithms, *Proc. of 46th annual Allerton Conference*, Allerton House, UIUC, Illinois, USA, pp. 1191–1198.

de Almeida, A.-L.-F., Favier, G. and Mota, J.-C.-M.: 2007, PARAFAC-based unified tensor modeling for wireless communication systems with application to blind multiuser equalization, *Signal Processing* **87**(2), 337–351.

Farber, B. and Zeger, K.: 2006, Quantization of multiple sources using nonnegative integer bit allocation, *IEEE Transactions on Information Theory* **52**, 4945–4964.

Gersho, A. and Gray, R. M.: 1992, *Vector quantization and signal compression*, Kluwer.

Henriksson, D. and Cervin, A.: 2005, Optimal on-line sampling period assignment for real-time control tasks based on plant state information, *Proc. IEEE Conference on Decision and Control*, pp. 4469–4474.

IEE: 2006, *IEEE 802.15.4 standard: Wireless Medium Access Control (MAC) and Physical Layer (PHY) Specifications for Low-Rate Wireless Personal Area Networks (WPANs)*.

Kibangou, A. and de Almeida, A.: 2010, Distributed PARAFAC based DS-CDMA blind receiver for wireless sensor networks, *Proc. of IEEE Int. Workshop on Signal Processing Advances for Wireless Comm. (SPAWC)*, Marrakech, Morocco.

Kibangou, A. and Favier, G.: 2009, Blind equalization of nonlinear channels using tensor decompositions with code/space/time diversities, *Signal Processing* **89**(2), 133–143.

Kruskal, J.: 1977, Three-way arrays: rank and uniqueness of trilinear decompositions, with application to arithmetic complexity and statistics, *Linear Algebra Applicat.* **18**, 95–138.

Ling, Q. and Lemmon, M. D.: 2005, Stability of quantized control systems under dynamic bit assignment, *IEEE Transactions on Automatic Control* **50**(5), 734–740.

Liu, X. and Goldsmith, A. J.: 2004, Wireless network design for distributed control, *Proc. IEEE Conference on Decision and Control*, pp. 2823 – 2829.

Luo, Z.-Q. and Liu, J.: 2006, Distributed signal processing in sensor netorks, *IEEE Signal Processing Magazine* **14**.

Mateos, G., Schizas, I. and Giannakis, G.: 2007, Consensus-based distributed least-mean square algorithm using wireless ad hoc networks, *Proc. of 45th annual Allerton Conference*, Allerton House, UIUC, Illinois, USA, pp. 568–574.

Nair, G. N., Fagnani, F., Zampieri, S. and Evans, R. J.: 2007, Feedback control under data rate constraints: An overview, *Proceedings of the IEEE* **95**(1), 108–137.

Nilsson, J.: 1998a, *Real-Time control systems with delays*, PhD thesis, Lund Institute of Technology. Ph.D. thesis.

Nilsson, J.: 1998b, Stochastic analysis and control of real-time systems with random time delays, *Automatica* **34**(1), 57–64.

Nion, D. and De Lathauwer, L.: 2008, An enhanced line search scheme for complex-valued tensor decompositions. Application in DS-CDMA, *Signal Processing* **88**(3), 749–755.

Park, P.: 2009, Protocol design for control applications using wireless sensor networks, *Technical Report TRITA-EE 2009:041*, Royal Institute of Technology (KTH). Licentiate thesis.

Park, P., Marco, P. D., Soldati, P., Fischione, C. and Johansson, K. H.: 2009, A generalized markov chain model for effective analysis of slotted IEEE 802.15.4, *Proc. IEEE conference on Mobile Adhoc and Sensor Systems*, pp. 130 – 139.

Pollin, S., Ergen, M., Ergen, S. C., Bougard, B., Perre, L., Moerman, I., Bahai, A., Varaiya, P. and Catthoor, F.: 2008, Performance analysis of slotted carrier sense IEEE 802.15.4 medium access layer, *IEEE Transactions on Wireless Communication* **7**(9), 3359–3371.

Schenato, L., Sinopoli, B., Franceschetti, M., Poola, K. and Sastry, S.: 2007, Foundations of control and estimation over lossy networks, *Proceedings of the IEEE* **95**(1), 163–187.

Seiler, P. and Sengupta, R.: 2001, Analysis of communication losses in vehicle control problems, *Proc. American Control Conference*, Vol. 2, pp. 1491–1496.

Sidiropoulos, N., Giannakis, G. and Bro, R.: 2000, Blind PARAFAC receivers for DS-CDMA systems, *IEEE Transactions on Signal Processing* **48**(3), 810–823.

Sinopoli, B., Schenato, L., Franceschetti, M., Poolla, K., Jordan, M. I. and Sastry, S. S.: 2004, Kalman filtering with intermittent observations, *IEEE Transactions on Automatic Control* **49**(9), 1453–1464.

Willig, A.: 2008, Recent and emerging topics in wireless industrial communication, *IEEE Transactions on Industrial Informatics* **4**(2), 102–124.

Xiao, L., Boyd, S. and Kim, S.-J.: 2007, Distributed average consensus with least-mean-square deviation, *Journal Parallel Distrib. Comput.* **67**, 33–46.

Xiao, L., Johansson, M., Hindi, H., Boyd, S. and Goldsmith, A.: 2005, Joint optimization of wireless communication and networked control systems, *Chapter in Switching and Learning, Springer Lecture Notes in Computer Science 3355* pp. 248–272.

Yu, M., Wang, L., Xie, G. and Chu, T.: 2004, Stabilization of networked control systems with data packet droupout via switched system approach, *IEEE International Symposium Computer Aided Control Systems Design*, pp. 362–367.

Zeger, K. and Manzella, V.: 1994, Asymptotic bounds on optimal noisy channel quantization via random coding, *IEEE Transactions on Information Theory* **40**(6).